Activity estimation of shielded or hidden radionuclides in emergency conditions

[1]H. Toivonen
[2]M. Granström
[2]G. Ågren
[3]G. Jónsson
[4]B. Møller
[5]P. Roos
[2]H. Ramebäck

[1]HT Nuclear, Finland
[2]FOI, Sweden
[3]IRSA, Iceland
[4]NRPA, Norway
[5]DTU Nutech, Denmark

Abstract

To perform a threat or risk estimation related to an unknown source, the following tasks need to be performed: detection of the source, identification of the nuclides involved, source localization and shield analysis around the source (attenuation). The present study focused on the shield analysis showing that the spectrum contains enough information to determine the attenuation of the photons in a material between the source and the detector.

The research brought together Nordic experts to use different gamma spectrometers in field conditions for improving readiness in a radiological or nuclear emergency. The field campaign was carried out in the FOI premises, Umeå, in August 2017 using HPGe, $LaBr_3$ and NaI spectrometers. For the attenuation calculation, the spectra were analysed in two ways: step analysis underneath a peak for single line emitters and peak area ratio analysis for multi-line emitters.

Careful calibrations were performed with Cs-137, Co-60 and Eu-152 sources for different attenuating materials (Pb, Fe, water and concrete) at a distance of 5 m and 10 m. Excellent data sets were generated. The results showed that in all cases the step response was linear. The peak ratio method worked well too, but the uncertainty analysis is a challenge.

The environment, the source-detector distance in particular, seems to have an impact on the step ratio (scattering). Furthermore, the comparison of the step analysis between Cs-137 and Co-60 showed that the parameters of the model have an energy dependency. These issues require more detailed studies, simulations and experimental work, before the adaption of the method for routine field work.

The measurement campaign was a great success showing that the properties of an unknown source in an unknown location in an unknown shield can be revealed in the field conditions. The results pave the way for realistic activity calculations which are the basis of risk estimation and well-justified countermeasures in emergency conditions.

Key words
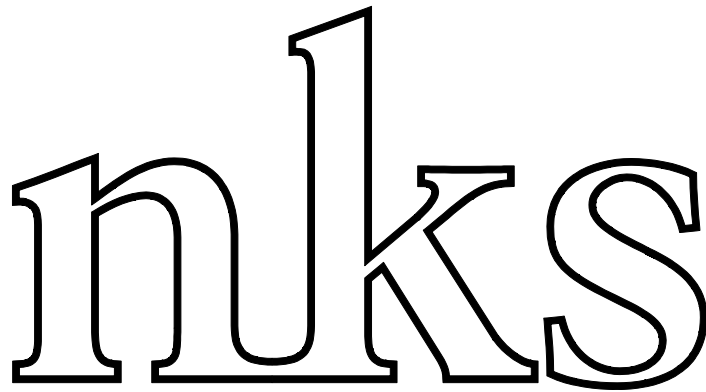
RadShield

Harri Toivonen, Micael Granström, Göran Ågren, Gisli Jonsson, Bredo Møller, Per Roos, Henrik Ramebäck

Activity estimation of shielded or hidden radionuclides in emergency conditions

RadShield

NKS project 2017

Coordinator:
Swedish Defence Research Agency, FOI (SE)
        Henrik Ramebäck

Participants:
HT Nuclear (FI)
        Harri Toivonen
Icelandic Radiation Safety Authority (IS)
        Gisli Jonsson
DTU Nutech (DK)
        Per Roos
NRPA (NO)
        Bredo Møller

Measurements:
        Micael Granström (SE), Göran Ågren (SE), Harri Toivonen (FI), Sakari Ihantola (FI), Jukka Härkönen (FI), Gísli Jónsson (IS), Benóný Þór Björnsson (IS)
Simulations with GEANT4:
        Sakari Ihantola (FI)
Observer:
        Yvonne Hinrichsen(DK)

Abstract

To perform a threat or risk estimation related to an unknown source, the following tasks need to be performed: detection of the source, identification of the nuclides involved, source localization and shield analysis around the source (attenuation). The present study focused on the shield analysis showing that the spectrum contains enough information to determine the attenuation of the photons in a material between the source and the detector.

The research brought together Nordic experts to use different gamma spectrometers in field conditions for improving readiness in a radiological or nuclear emergency. The field campaign was carried out in the FOI premises, Umeå, in August 2017 using HPGe, LaBr$_3$ and NaI spectrometers. For the attenuation calculation, the spectra were analysed in two ways: step analysis underneath a peak for single line emitters and peak area ratio analysis for multi-line emitters.

Careful calibrations were performed with Cs-137, Co-60 and Eu-152 sources for different attenuating materials (Pb, Fe, water and concrete) at a distance of 5 m and 10 m. Excellent data sets were generated. The results showed that in all cases the step response was linear. The peak ratio method worked well too, but the uncertainty analysis is a challenge.

The environment, the source-detector distance in particular, seems to have an impact on the step ratio (scattering). Furthermore, the comparison of the step analysis between Cs-137 and Co-60 showed that the parameters of the model have an energy dependency. These issues require more detailed studies, simulations and experimental work, before the adaption of the method for routine field work.

The measurement campaign was a great success showing that the properties of an unknown source in an unknown location in an unknown shield can be revealed in the field conditions. The results pave the way for realistic activity calculations which are the basis of risk estimation and well-justified countermeasures in emergency conditions.

Symbols

- activity of the source (Bq) a_s

- apparent activity of the source (Bq) a_a

- count rate at energy E $C(E)$

- yield of the photons $\gamma(E)$

- energy of the photons (keV) E

- source-detector distance (m) r

- reference distance (m) r_0

- efficiency of the detector $\varepsilon(r,E)$

- efficiency at reference distance $\varepsilon(r_0,E)$

- attenuation coefficient of air (1/m) $\mu_{air}(E)$

- attenuation coefficient of shielding (1/cm) $\mu_i(E)$

- exponential attenuation factor in shielding $F(E)$

- thickness of the attenuators (cm) x_i

- effective lead thickness (cm) X_{Pb}

1. Introduction

Activity estimation of radioactive sources is one of the basic concepts in radiation safety as well as after nuclear security events. In laboratory conditions this is a well-established technique. However, in field appllctions the measurement is much more complex because of an unknown measurement geometry, including shielding between the source and the detector. The source could be heavily masked, the signal being small, but the actual activity might still be very large. To draw correct conclusions from the spectrometric measurements, new analysis methods have to be developed.

The spectrum baseline contains information about the shielding of the source. The analysis of the continuum provides an interesting approach to provide crucial information for the activity estimation. The present research consortium demonstrates the problem and provides initiatives for better analysis of unknown gamma emitters which are either sealed or behind complex obstacles, such as a concrete wall.

The spectrum analysis is performed in two ways: (1) step analysis underneath each peak and, (2) traditional peak analysis resolving individual peaks and then determining their peak area ratios for the attenuation calculation.

The research brought together experts from Sweden, Finland and Iceland to use different gamma spectrometers in the field conditions for improving readiness in a radiological or nuclear accident. The field campaign was carried out in the FOI premises, Umeå, in August 2017.

2. Step ratio for shielding analysis

The step ratio, *SR(E,t)*, is defined as

$$SR(E,x) = \frac{H(E,x)}{A(E,x)} \tag{2.1}$$

where

- *H(E,x)* is the total height of the step; the unit of *H* is 1/keV.
- *A(E,x)* is the area of the peak located at energy *E* in a measurement system where certain attenuating material with thickness *x* is located between the source and the detector.

To avoid the impact of interfering radionuclides, *SR* should be calculated using data as near to the peak as possible (see Figure 2.1). The step ratio *SR* can be measured as a function of material thickness. This calibration curve can then be used for calculating the unknown thickness of the attenuating material, is strictly true only for similar environments for the calibration and the field measurements.
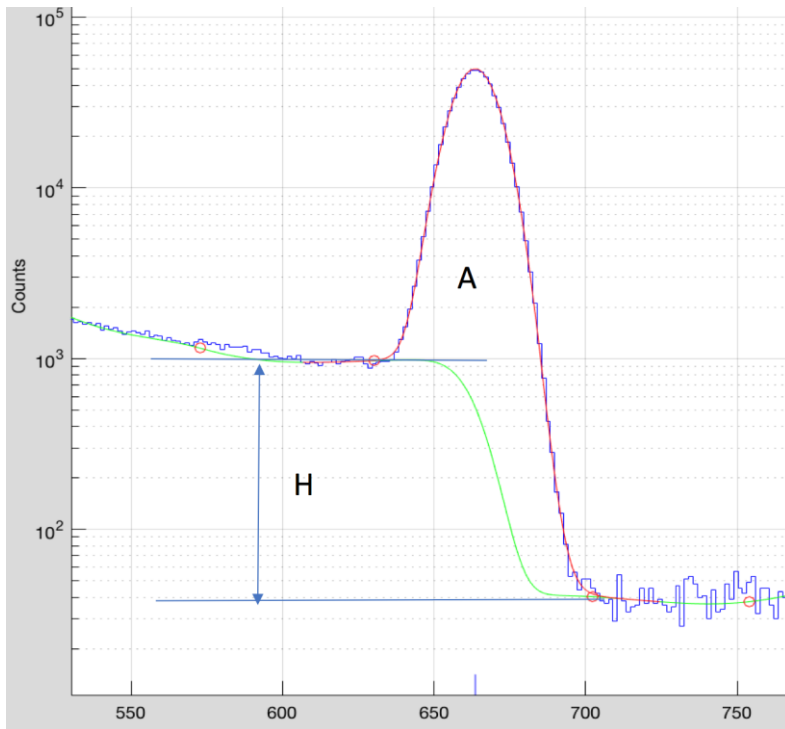
Figure 2.1 Definition of step height H (1/keV). H can also be understood as an area of a rectangle having width of 1 keV. Measurement ID 2.
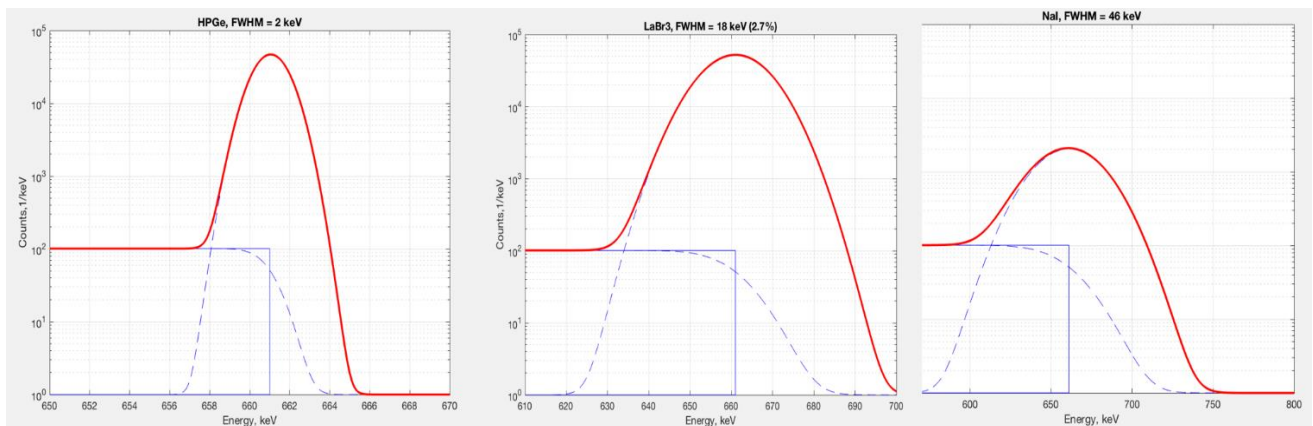
Figure 2.2 Step underneath a Gaussian peak as a function of detector resolution. The step is an inverse erf function with the same shape parameter as the peak itself. SR =0.001; (H = 100, A =100000). The figure shows the convolution of a step (rectangle) and energy peak at 661 keV (delta function) with a Gaussian resolution function characteristic to different detectors.

Figure 2.2 shows the response of the detector to the step underneath the ^{137}Cs peak (661 keV). The high resolution of the HPGe detector allows the step analysis near the peak; the counts below 656 keV are free of peak interference whereas the same figures for LaBr$_3$ and NaI are 632 keV and 590 keV, respectively. In practise, far away from the main peak, there may be interfering peaks, and therefore the step analysis is very challenging for the low-resolution detectors.

3. Peak area ratio for shielding analysis

For an unshielded point source, the efficiency of the detector is[1]

$$\varepsilon(r,E) = \left(\frac{r_0}{r}\right)^2 e^{-\mu_{air}(E)(r-r_0)} \varepsilon(r_0, E) \tag{3.1}$$

where $\varepsilon(r_0,E)$ is the efficiency at a reference distance r_0 (e.g. 5 m).

The count rate $C_A = C_A(r,E_A)$ for energy E_A measured at a distance r, is

$$C_A = a_S \gamma_A \varepsilon(r, E_A) F(E_A) \tag{3.2}$$

where a_S is the activity of the source, γ_A the photon emission probability at energy E_A and $F(E_A)$ describes the attenuation induced by the materials, here Pb is considered, between the source and the detector:

$$F(E_A) = e^{-\sum_i \mu_i(E_A)x_i} = e^{-\mu_{Pb}(E_A)X_{Pb}}. \tag{3.3}$$

Here an effective attenuation thickness X_{Pb} is introduced in a (hypothetical) geometry where all the external material between the source and the detector is one type of material, such as lead. Of course, this can be converted to effective thickness of any material, concrete for example.

A good practice is to first calculate an apparent activity a_a from Equation (3.2) by omitting the shielding factor $F(E_A)$, and then perform a review for all measured results at different locations. This analysis may reveal measurements which are more reliable than others. The shielding analysis is independent from the activity calculation. The last step is to combine these two analyses; in essence, $a_S = a_a/F$.

Let us now calculate the ratio of two peak areas recorded at the energies E_A and E_B:

$$P = \frac{C_A(r,E_A)}{C_B(r,E_B)} = \frac{\gamma_A}{\gamma_B} \frac{\varepsilon(r,E_A)}{\varepsilon(r,E_B)} e^{-[\mu_{Pb}(E_A)-\mu_{Pb}(E_B)]X_{Pb}}. \tag{3.4}$$

Introducing the unknown distance r from Equation (3.1) gives

$$P = \frac{\gamma_A}{\gamma_B} \frac{\varepsilon(r_0,E_A)}{\varepsilon(r_0,E_B)} e^{-[\mu_{air}(E_A)-\mu_{air}(E_B)](r-r_0)} e^{-[\mu(E_A)-\mu(E_B)]X_{Pb}}. \tag{3.5}$$

Therefore

---

[1] The analysis is taken from an unpublished document "Source Activity Calculation from Two or More Peaks of a Nuclide in an Unknown Geometry", H. Toivonen, HT Nuclear Ltd, 2017.

$$X_{Pb} = -\frac{\log(K)}{\mu_{Pb}(E_A)-\mu_{Pb}(E_B)} - \frac{[\mu_{air}(E_A)-\mu_{air}(E_B)](r-r_0)}{\mu_{Pb}(E_A)-\mu_{Pb}(E_B)} \qquad (3.6)$$

where

$$K = \frac{C_A(r,E_A)}{C_B(r,E_B)}\frac{\gamma_B}{\gamma_A}\frac{\varepsilon(r_0,E_B)}{\varepsilon(r_0,E_A)}. \qquad (3.7)$$

Ignoring the energy dependency of the absorption in air gives

$$X_{Pb} \approx -\frac{\log(K)}{\mu_{Pb}(E_A)-\mu_{Pb}(E_B)}. \qquad (3.8)$$

This is a good approximation in most cases. For example, for ^{60}Co, the difference in predicted shielding thickness (0.67×10^{-4} Δr) is less than 0.67 mm for $\Delta r = r - r_0 = 10$ m. However, if the source is very far away from the reference point, the correct Equation (3.6) must be used with an assumed distance r. In addition, if the energies E_A and E_B are close to each other, then also the attenuation coefficients are close to each other, and consequently, considerable uncertainty may be introduced (see Chapter 7).

The method described above does not require any calibration measurements for shield thickness analysis. However, the method depends on the ratio of counting efficiencies $\varepsilon(r_0,E_A)/\varepsilon(r_0,E_B)$ and on the difference between the linear attenuation coefficients $\mu(E_A) - \mu(E_B)$; also the yield ratio $\gamma(E_A)/\gamma(E_B)$ may play a role albeit with ^{60}Co this is not an issue.

The efficiency calibration is very difficult to perform better than with an uncertainty of 5%. But since we are interested in the ratio of two efficiencies the uncertainty of this ratio may be significantly lower than 5% due to possible correlations. However, this is something that has to be evaluated in a future project.

The mass attenuation coefficients (cm^2/g) for different materials have been known for a long time. They are listed for ^{60}Co in Table 3.1. They are intended for a narrow beam application. However, the present study deals with broad beams with heavy shielding. Then the contribution of the Rayleigh scattering must be subtracted from the total attenuation coefficients. In practice this has an impact for Pb shields (and U shields) with thickness more than 5 cm. Further uncertainty is introduced through the density of the material. Therefore, the predicted linear attenuation coefficients cannot be regarded as high-precision constants.

The problems described above are avoided by measuring a calibration curve, i.e. by measuring the peak area ratio as a function of material thickness. This approach has an auxiliary advantage, namely analysis method. When the calibration measurements and the unknown source measurements are analyzed with the same software and with the same procedure, the systematic uncertainties related to peak area quantification will cancel out. For high precision shield analysis, a calibration curve is a fundamental requirement.

For any material, having a thickness of x, the equation 3.4 can be written as

$$P = ae^{bx} \qquad (3.9)$$

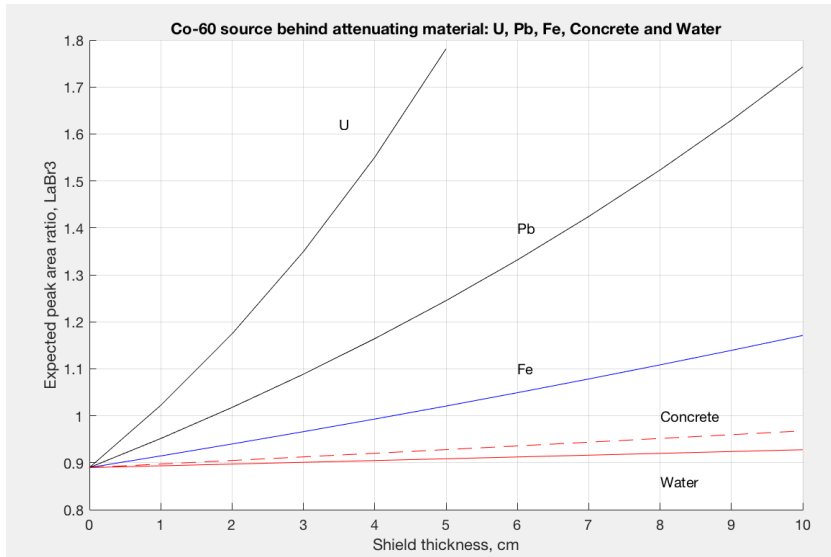where a and b are coefficients to be determined by least squares fitting. For the expected response, see Figure 3.1.

Figure 3.1. Expected peak area ratio (1332/1173) in different attenuating materials for [60]Co. The dynamic range for concrete and water is very small, thus making it difficult to apply for shield thickness analysis. The analysis is based on narrow beam assumption.

Table 3.1. Linear attenuation coefficients of ^{60}Co gamma rays. Mass attenuation coefficient in parenthesis (cm^2/g). Linear interpolation from NIST data was used to calculate the attenuation coefficients for a specific energy. For broad beam applications, a correction for Rayleigh scattering must be performed.

Nuclide Energy (keV)		**Narrow beam attenuation coefficients (1/cm)**					
	Material Density (g/cm^3)	**Air**, T = 20 ^{0}C 1.2041E-3	**Pb** 11.35	**U** 19.1	**Fe** 7.8	**Water** 1.0	**Concrete** 2.2
Co-60	Data source						
1173	NIST(*)	0.7097E-4 (0.05894)	0.7098 (0.0625)	1.3064 (0.0684)	0.4328 (0.0555)	0.0655 (0.0655)	0.1324 (0.0602)
1332		0.6644E-4 (0.0553)	0.6426 (0.0566)	1.1676 (0.0611)	0.4054 (0.0520)	0.0614 (0.0614)	0.1240 (0.0564)

* https://physics.nist.gov/PhysRefData/XrayMassCoef/tab3.html

From equation (3.9) we get the shield thickness and its uncertainty Δx:

$$x = \frac{\ln(\frac{P}{a})}{b} \tag{3.10}$$

and

$$\Delta x = \frac{1}{100b}\left|\frac{\Delta P}{P}\right| \tag{3.11}$$

where *ΔP/P* is the relative uncertainty of the peak area ratios in percent.

4. Irradiation setup

Gamma spectrometric calibration measurements were performed with high-activity sources.

^{137}Cs source (Isotope Products Laboratories, USA).

This source is made from CsCl in a ceramic matrix, encapsulated in stainless steel. The source activity at the reference date was 3.5 GBq with an uncertainty of 5% (95% CI). The reference date was 1st October 1987. The activity on the day of the experiment was 1.8 GBq.

^{60}Co source (Tech/Ops, USA).

This source is a radiography source with a mechanical system to expose the activity by winding out the source in a hose. The source activity at the reference date was 407 GBq. The reference date was 3rd February 1984. The activity on the day of the experiment was 4.95 GBq.

^{152}Eu source (Eckert & Ziegler, Germany).

This source is made from porous glass, encapsulated in stainless steel. The source nominal activity at the reference date was 740 MBq, activity tolerance ± 15%. The reference date was 15th January 2013. The activity on the day of the experiments was 585 MBq.

The measurement geometry was realistic from the point of view of field operations, including accidents. The source-detector distances were typically 5 m or 10 m, but a distance of 70 m was sometimes used. Measurements were performed with different shielding materials between the source and the detector (Fe, Pb, concrete and water). For details, see Appendix 1 for controlled measurements at FOI (tent: 10 x 15 m^2).

5. Simulations

Simulations were performed with Geant4 software, code version 10.03.p01. The physics models activated were: G4DecayPhysics, G4RadioactiveDecayPhysics and G4EmStandardPhysics.

The simulation geometry consisted of a large volume of air where the detector, source and its shield were placed. The shield was a 1m x 1m slab; thickness and material were varied. The source used was a point source in the centre of the geometry. The distance from the source to the detector was measured to the closest point on the surface of the detector. The detector and the shield were aligned such that the gamma rays reaching the centre of the active volume of the detector without interactions travelled perpendicular through the shield.

The simulations were primarily made for Environics RanidPro 200 detector with a 1.5" x 1.5" LaBr$_3$ crystal. For the efficiency curve, see Figure 5.1. Some of the simulations were also repeated for Ortec Detective with a 50 mm x 30 mm HPGe crystal (results not shown) which has quite similar efficiency response albeit much better resolution. However, the detector resolutions were not simulated or taken into account in the data analysis (no need for the present theoretical analysis).
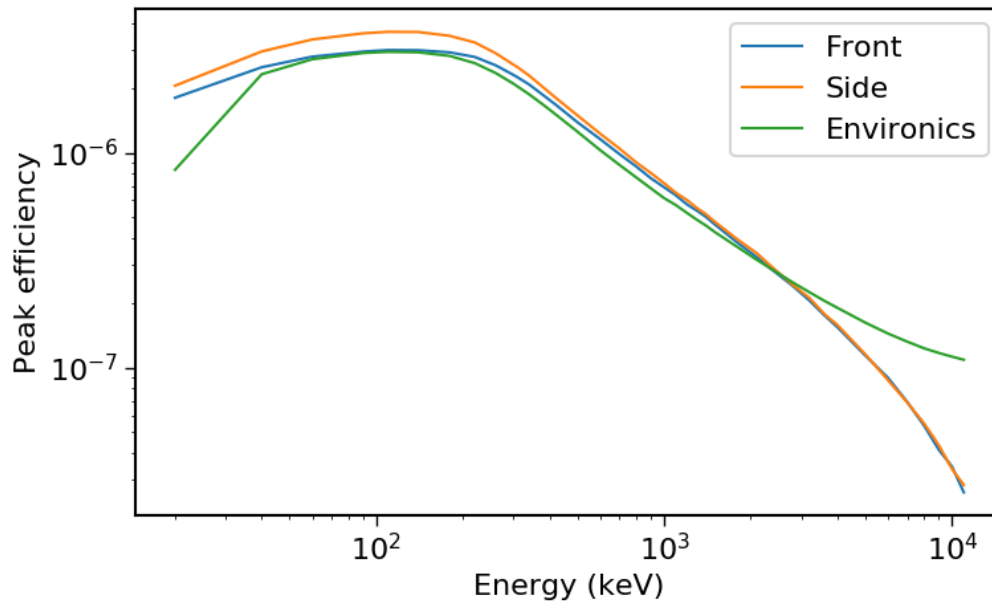
Figure 5.1. Simulated peak efficiencies for the Environics RanidPro 200 LaBr$_3$ detector at 5.0 m source-detector distance. The efficiency curve reported by Environics is given for comparison. The curves are near each other at the energy interval relevant to the present study (661 keV – 1332 keV). For Co-60, ε(5 m, 1173 keV) = 0.537E-6 and ε(5 m, 1332 keV) = 0.478E-6.

The simulated step ratios as a function of shield thickness are shown in Figure 5.2 for different materials in front of a ^{137}Cs source.
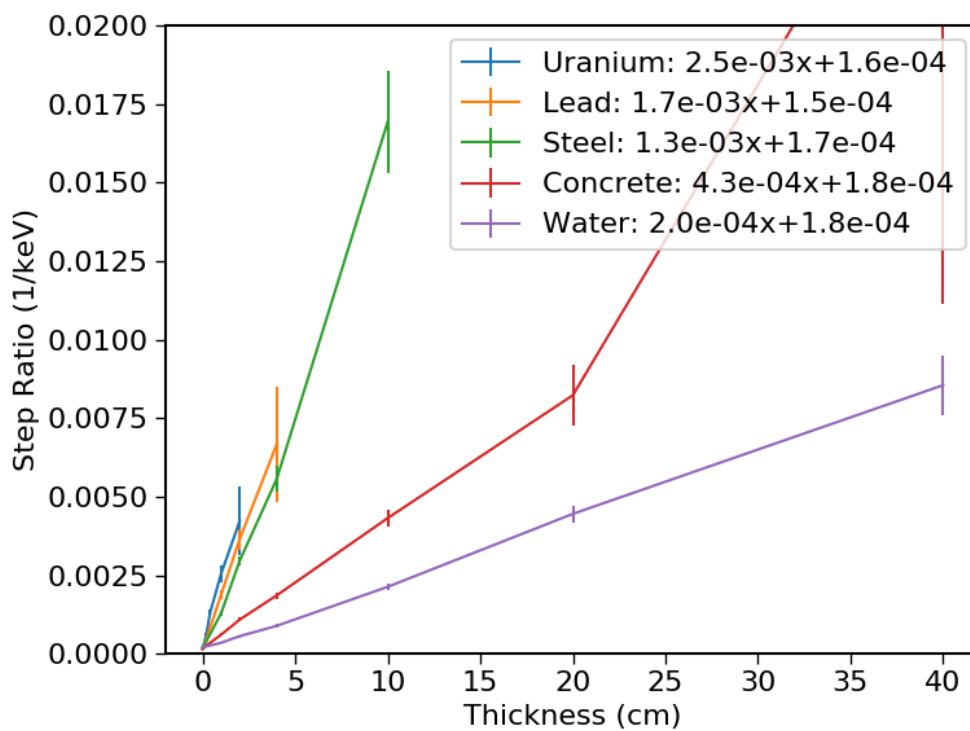
Figure 5.2. Simulated step ratio at 662 keV for a LaBr₃ detector as a function of shield thickness. The numbers in the legend present least squares fit to the data points. For comparison with the measurements, see Chapter 6.2.1

5.1 Impact of the geometry

In the ideal situation, the changes in the recorded spectrum would only depend on the thickness of the shield and not on other geometrical factors, such as the geometry of the shield or structures that are not in the line-of-sight from source to detector.

Figure 5.3 shows the gamma-ray spectrum of a LaBr₃ detector through a 5 cm thick concrete shield when the source is either isotropic or collimated to a 5-degree angle towards the detector. The source-detector distance was 1 m and the shield located halfway between the source and the detector. As can be seen, the collimation has a huge impact on the shape of the spectrum. This indicates that the shape of the spectrum may not just depend on the thickness of the shield, but also on other geometrical factors.
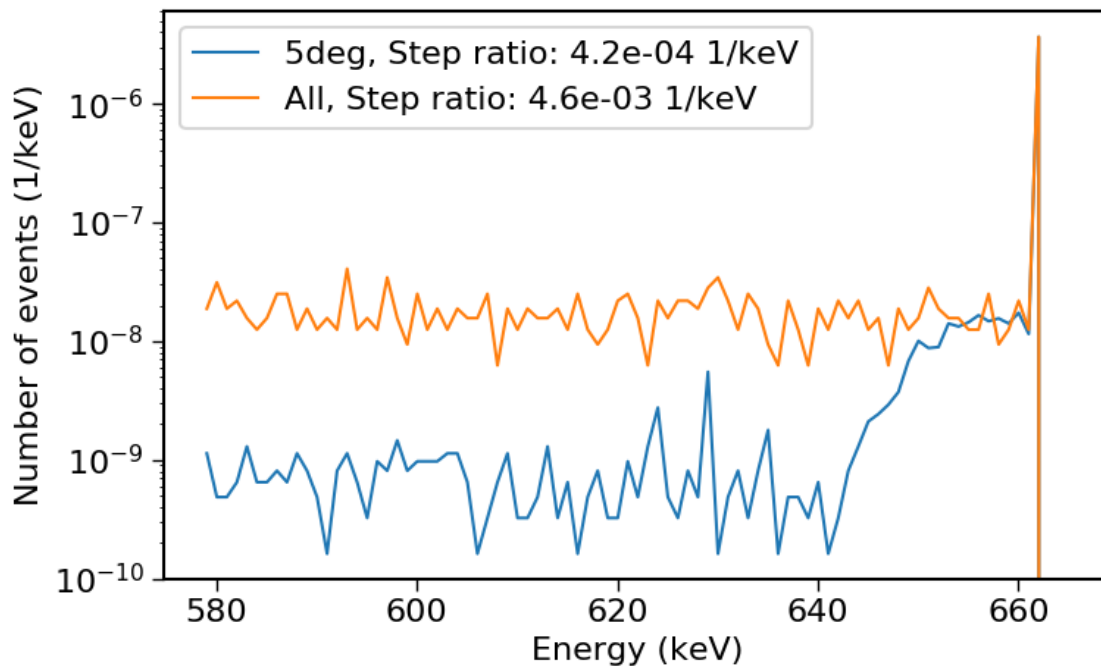

Figure 5.3. Simulated ^{137}Cs spectra for a LaBr detector at 1.0 m distance from the source behind a 5 cm thick concrete shield. The gamma source used is either collimated to a 5 degree cone towards the detector (5deg) or isotropic (All).

It is worth noticing that the step less than 10 keV below the peak is at the same height in both spectra, indicating that the spectrum more than 10 keV below the peak is caused by scatter into angles larger than 10 degrees.

The energy of the scattered photon in Compton scattering is given by the equation

$$E' = \frac{1}{1/E_0[1-\cos(\theta)]+1/E} \qquad \qquad 2)$$

With a peak energy of 661 keV, the electron rest mass (E_0=511 keV) and maximum scatter angle (θ=10 deg), we see that the minimum energy of scattered gamma-rays is 649 keV. This is in line with the simulation and confirms that the step on the left side of the photo peak is caused by Compton scattering.

Figure 5.4 presents how the spectrum changes if both the source and the detector are on a floor simulated with a 0.5 m thick slab of concrete. Even though the influence of the floor is clearly visible, the step on the left side of the photo peak is still quite small. Similar step would be caused by 1.5 mm of lead shield, inducing a 30% drop in the peak efficiency.
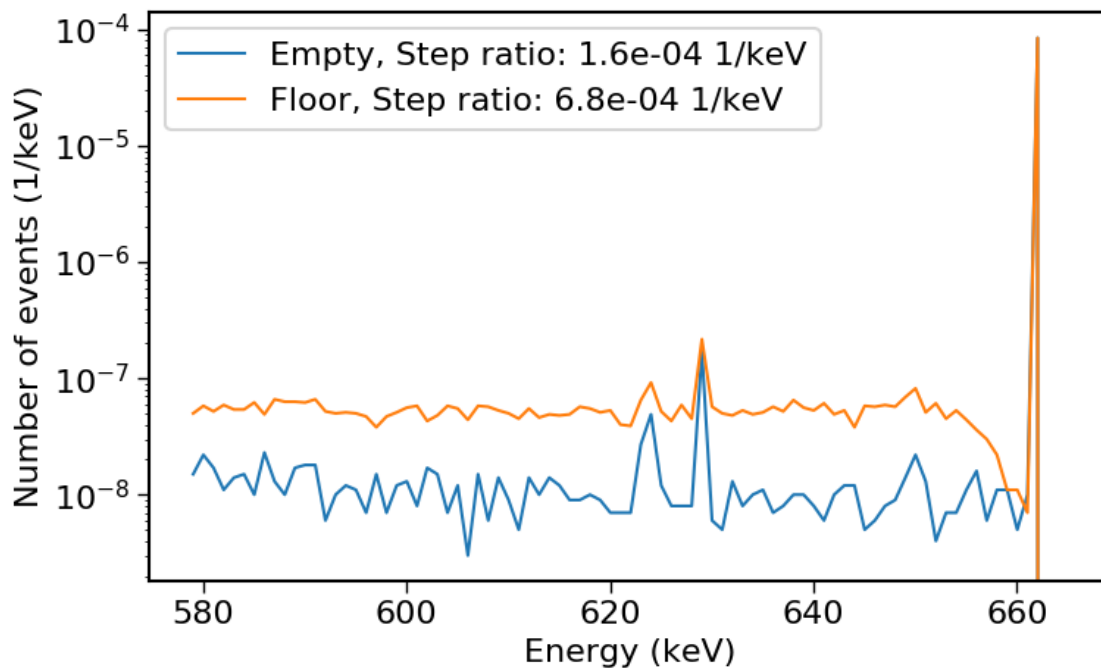

Figure 5.4. Simulated Cs-137 spectra for a LaBr$_3$ detector at 0.5 m distance from the source when both the source and the detector are on a concrete floor.

5.2 Impact of the detector

In the ideal case, the step ratio would only depend on the shield but not on the detector itself. This would mean that the same step ratio data could be used for the analysis of spectra recorded with different types of detectors.

The dependence of the step ratio on the detector was studied by analysing the step ratio as a function of the lead shield thickness both for the LaBr$_3$ and HPGe detectors. The result is shown in Figure 5.5. As can be see, the slopes of the step ratio curves recorded with both detectors are very similar but the offset is somewhat different. This indicates that the slope of the curve is a property of the shield but the offset is caused by the scattering from the detector itself (detector casing, dead layer etc). However, conclusive analysis would require simulations with different detector geometries and better statistics.
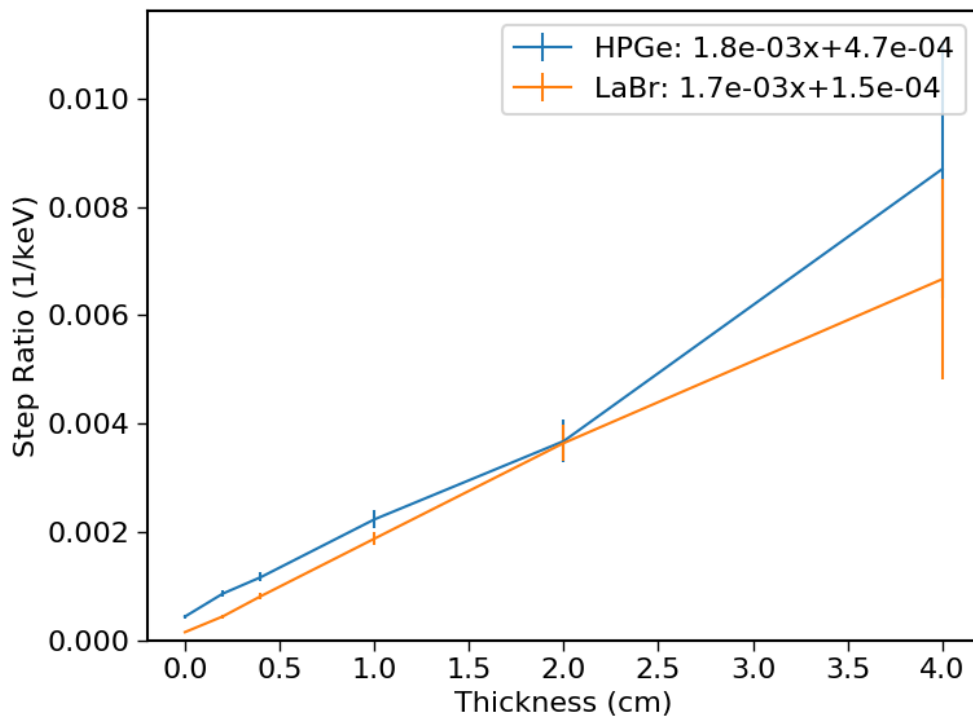
Figure 5.5. ^{137}Cs step ratio for the LaBr$_3$ and HPGe detectors as a function of the thickness of the lead shield. The response seems to be independent of the type of the detector.

6. HPGe measurements

6.1 Detection system

The measurements with the HPGe detector were performed by the Swedish team. For the experiments two DetectiveEX (Ortec, USA) HPGe detectors were used. Since the detectors are mechanically cooled with a Stirling-type cryocooler there is no need for liquid nitrogen. The detectors can both work as stand-alone or can be controlled with an external computer *via* an usb interface.

The specifications of the detectors:

- Crystal Diameter: 50 mm
- Crystal Length: 30 mm

The detector resolutions are approx. 2.0 keV at 662 keV and 2.5 keV att 1332 keV. The spectra were recorded using the software GammaVision (Ortec, USA) and the measurement was stopped when the total counts in the main peaks were 10 000 counts.

6.2 Analysis of the ratio of the baseline step to peak area

The step ratio parameters for the 661 keV peak of ^{137}Cs are given in Table 6.1. For the measurements, see Appendix 2.

The step ratio parameters for the 1332 peak of Co-60 are listed in Table 6.2. For the measurements, see Appendix 2.

Table 6.1. Step ratio parameters for 661 keV peak of ^{137}Cs. Measurement @ 5 m. Linear function: SR = p1*x+p2. Variable *x* (thickness) in units of cm; 95% confidence interval in parenthesis.

	Material	p1 (1/cm) (x 10^{-3})	p2 (x 10^{-3})
Detector 1	Fe	1.34 (1.26-1.41)	2.00 (1.63-2.36)
Detector 2	Fe	1.27 (1.22-1.32)	1.52 (1.26-1.78)
Detector 1	Concrete	0.37 (0.35-0.38)	1.85 (1.76-1.93)
Detector 2	Concrete	0.34 (0.29-0.40)	1.42 (1.08-1.76)

Since there were only one known thickness for the Pb shielding of Cs-137 we did not perform a step analysis of that.

Table 6.2. Step ratio parameters for the 1332 keV peak of ^{60}Co. Measurement @ 10 m. Linear function: SR = p1*x+p2. Variable *x* (thickness) in units of cm; 95% confidence interval in parenthesis.

	Material	**p1 (1/cm)** (x 10^{-3})	**p2** (x 10^{-3})
Detector 1	Pb	0.38 (0.33-0.42)	1.43 (1.19-1.67)
Detector 2	Pb	0.38 (0.34-0.42)	1.22 (1.02-1.42)
Detector 1	Fe	0.39 (0.38-0.39)	1.37 (1.35-1.39)
Detector 2	Fe	0.38 (0.36-0.39	1.17 (1.09-1.24)

6.3 Analysis of the ratio of two peak areas

The peak area ratios for the 1408/779 keV peaks of the Eu-152 spectrum are listed in table 6.3. The shielding material used was iron (Fe). For the measurements, see Appendix 2.

The peak area ratios for the 1332/1173 keV peaks of Co-60 are listed in table 6.4. The shielding material was lead (Pb). For the measurements, see appendix 2.

Table 6.3. Peak area ratios for the 1408/779 keV peaks of ^{152}Eu. Measurement @ 5 m. Counting statistics uncertainty in parenthesis (k=2).

Fe thickness (cm)	Detector 1	Detector 2
0	0.954 (0.027)	0.934 (0.029)
1	1.103 (0.052)	1.043 (0.055)
3	1.453 (0.086)	1.468 (0.103)
5.5	1.988 (0.212)	1.987 (0.277)

Table 6.4. Peak area ratios for the 1332/1173 keV peaks of ^{60}Co. Measurement @ 10 m. Counting statistics uncertainty in parenthesis (k=2).

Pb thickness (cm)	Detector 1	Detector 2
0	0.897 (0.009)	0.906 (0.010)
1	0.940 (0.010)	0.947 (0.012)
2.5	1.036 (0.014)	1.040 (0.017)
5	1.169 (0.029)	1.197 (0.036)
10	1.547 (0.129)	1.549 (0.180)

7. LaBr₃ measurements

7.1 Detection system

The measurements with the LaBr₃ detector were performed by the Finnish team. The instrument was a RanidPro200 backbag, Environics Ltd. The detector has a resolution of 18.0 keV (2.7%) at 661 keV and 26.7 keV (2.0%) at 1332 keV. The efficiency of the detector was calibrated for a source-detector distance of 5 m. Spectra are recorded in a local database (Linssi) in intervals of 500 ms. There are powerful tools to create summation spectra for any time interval. This provides complete control of the optimum start and stop time of data acquisition. The spectra can be transmitted wirelessly to a remote database (reachback centre) but this capability was not used in the field work at FOI.

RanidPro200 backbag contains a source localizer, known as RanidSOLO, which gives the direction from the detector to the source with a precision of a few degrees. The localizer also gives the source-detector distance when two measurements are performed in different locations (two vectors). The method is independent of different attenuation at different directions. The source localizer removes much of the uncertainty in the activity analysis since the uncertainty related to the distance can be eliminated.

The LaBr₃ detector has an internal contamination (^{138}La) which interferes with the baseline and peak area analysis of ^{60}Co peaks. If good counting statistics is available this has no significant impact on the results. However, with poorer counting statistics, as is seen in a measurement with 10 cm Pb shielding, the impact is of importance (see Figure 7.1).
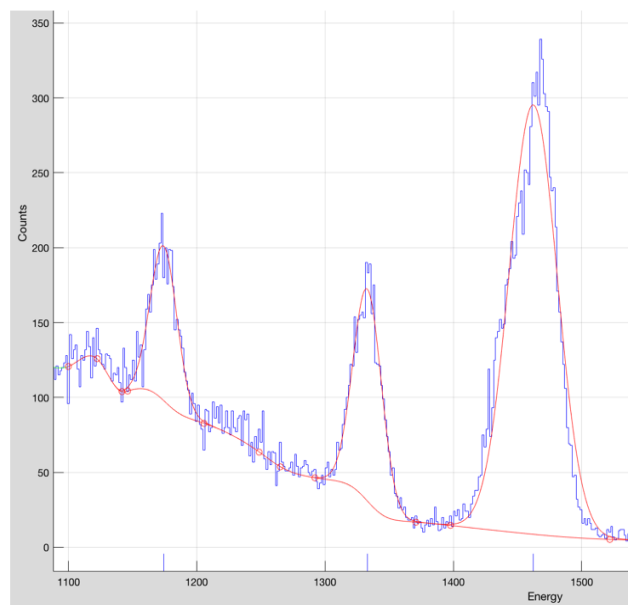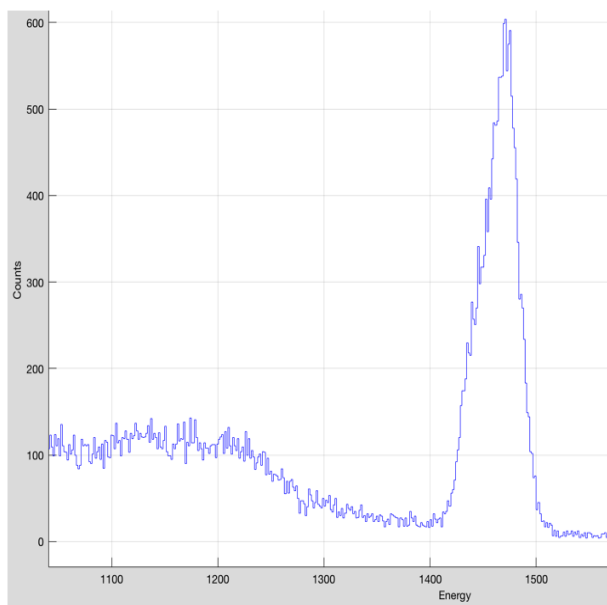
Figure 7.1. Interference of internal contamination of LaBr$_3$ detector with the Co-peaks. Left: background spectrum; right ^{60}Co source with 10 cm Pb shielding. The 1173 keV peak is located above a small lump caused by the internal contamination.

7.2 Analysis of the ratio of the baseline step to peak area

The step ratio parameters are given in Tables 7.1 for the 661 keV peak of ^{137}Cs. For the measurements, see Appendix 3.

Table 7.2 gives the measured step parameters for the 1332 keV peak of ^{60}Co. It is evident that the step height depends on the initial energy of the photons, i.e., the step is more prominent at lower energies. In fact, some earlier studies with air filter samples[2] indicate that the step increases heavily when the photons have energies below 200 keV.

Table 7.1. Step ratio parameters for 661 keV peak of ^{137}Cs. Measurement @ 5 m, simulation in air @ 0.5 m. Linear function: SR = p1*x+p2. Variable *x* (thickness) in units of cm; 95% confidence interval in parenthesis; unk = unknown.

Material	p1 (1/cm) (x 10^{-3})	p2 (x 10^{-3})
Pb	1.65 (unk)	1.0 (unk)
Fe	1.53 (1.49-1.57)	0.85 (0.65-1.04)
Concrete	0.38 (0.17-0.57)	0.99 (0-2.2)

---

[2] H. Toivonen. Reference Manual of Radionuclide Analysis and Evaluation Software Aatami, CTBTO 2007.

Table 7.2. Step ratio parameters for the 1332 keV peak of ^{60}Co. Measurement @ 10 m. Linear function: SR = p1*x+p2. Variable *x* (thickness) in units of cm; 95% confidence interval in parenthesis.

Material	p1 (1/cm) (x 10^{-3})	p2 (x 10^{-3})
Pb	0.46 (0.31-0.62)	0.49 (0.25-0.73)
Fe	0.33 (0.30-0.36)	0.55 (0.41-0.69
Water	0.054 (0.048-0.62)	0.46 (0.33-0.58)

7.3 Analysis of the ratio of two peak areas

The analysis of shield thickness can suffer from considerable uncertainty, if the basis of the approach is the attenuation theory, as given in Chapter 3. Figure 9 in Appendix 3 shows that the predicted response, based on ideal narrow-beam attenuation, differs from the measured response for Pb. The linear attenuation coefficients (see Table 3.1) are near each other for the peaks of Co-60, and therefore the uncertainty of the difference $\mu(E_A) - \mu(E_B)$ may be considerable. Note, that the direct use of total attenuation coefficients $\mu(E)$ is not valid in the analysis of thick shields.

The accuracy of the peak ratio analysis is greatly improved by calibration measurements using different attenuation materials (see Appendix 3, section C). In Table 7.1 the fitting parameters are compared against the expected value (difference between the linear attenuation coefficients). The parameter *a* has a value near 0.913 (Pb and Fe results from fitting) whereas its expected value, the ratio $\varepsilon(r_0,E_A)/\varepsilon(r_0,E_B)$, is 2.6% smaller (data from the efficiency calibration of the detector). The parameter *b* agrees reasonable well for Fe but not for Pb and water. For Pb, the reason is the direct use of total attenuation coefficients (see above) whereas for water, the attenuation was quite low, and consequently, the response function is flat (see Appendix 3, Figure 8) containing unprecise data.

Table 7.2. Peak area ratio parameters *a* and *b* in Eq. (3.9) for ^{60}Co. Measurement @ 10 m. The expected values are taken from Table 3.1.

Material	a Expected	a Fitted	b Expected	b Fitted
Pb	0.8896	0.9134	0.0672	0.05469
Fe	0.8896	0.9127	0.0274	0.02600
Water	0.8896	0.9195	0.0041	0.00284

7.4 Localization of unknown sources

Localization principle

RanidSOLO has and automated rotating attenuator which provides the direction of the source. The localization method is fully automated and can be achieved with high precision (a few degrees). When two measurements are made in two locations, also the source-detector distance can be determined although there would be asymmetrical attenuation of photons. The measurement principle is given in Figure 7.2.
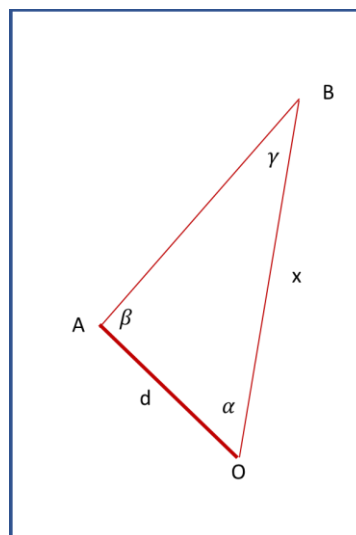
Distance x

1. Define baseline OA
2. Measure distance OA
3. Measure angels α and β
4. Calculate distance x:

$$\gamma = 180 - \alpha - \beta$$

$$x = \frac{\sin(\beta)}{\sin(\gamma)} d$$

Figure 7.2. Source localization with RanidSOLO.

Two unknown sources with unknown shielding were placed somewhere outside the FOI tent. The task was to identify and localize the sources, and then to estimate their shielding properties, and finally to get an understanding of the activities of the sources. The spectrometric measurements revealed immediately that the two sources were ^{60}Co and ^{137}Cs.

Localization of the unknown sources

The measurement geometry and the localization results are given in Figures 7.3 – 7.7.

Measurements

Tent 10x15 m²

Basic setup (m)
a = 2.4
b = 3.6
OA = 5.0 (Co)
OB = 13.3 (Cs)
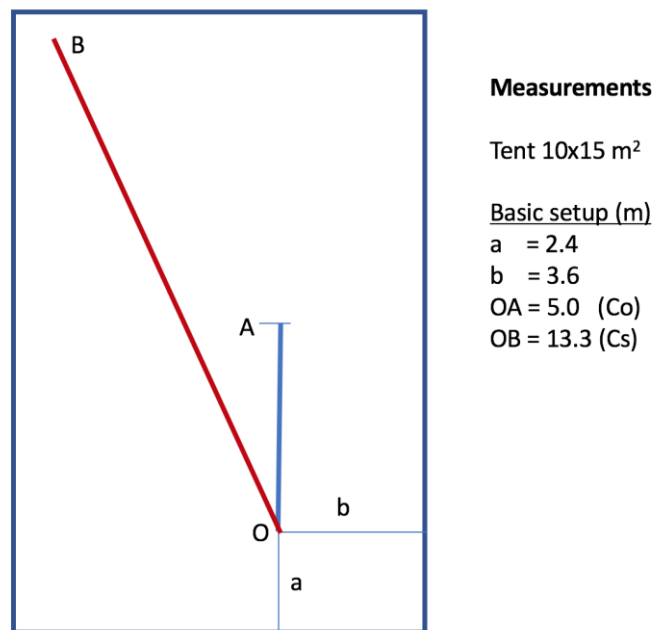
Figure 7.3. Measurement setup for the unknown sources which were outside the tent. The ^{60}Co source was studied in measurement location O and A and the ^{137}Cs source in location O and B. The distances were measured with a laser pointer.
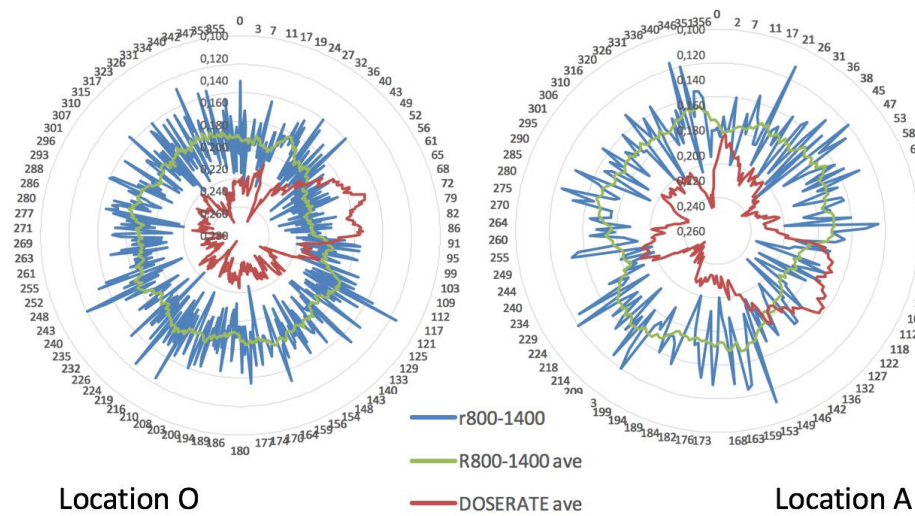
Location O

r800-1400
R800-1400 ave
DOSERATE ave

Location A

Figure 7.4. Count rate from a ^{60}Co source in polar plot at energy interval 800 – 1400 keV. The doserate is plotted in such a way that the highest values are pointing outwards. The doserate varied between 0.21 - 0.24 μSv/h.
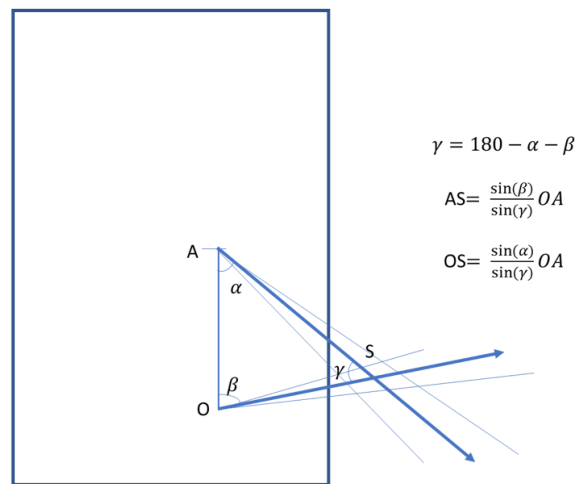

$$\gamma = 180 - \alpha - \beta$$

$$AS = \frac{\sin(\beta)}{\sin(\gamma)} OA$$

$$OS = \frac{\sin(\alpha)}{\sin(\gamma)} OA$$

Figure 7.5. Localization of the ^{60}Co source. RanidSOLO provided the directional angles: α = 58˚ ±2˚ and β = 72˚ ± 2˚. Therefore, the distances were AS = 6.2 m ± 0.5 m and OS= 5.5 m ± 0.5.
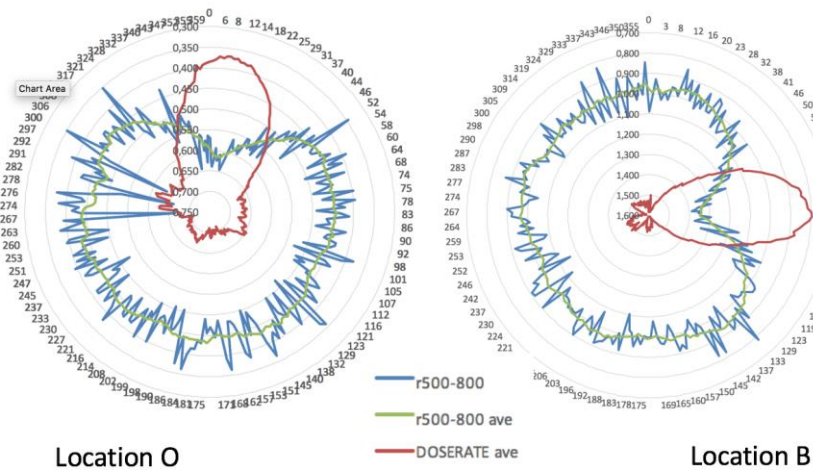
Figure 7.6. Count rate of a ^{137}Cs source in a polar plot at energy interval 500-800 keV. The dose rate is plotted in such a way that the highest values are pointing outwards. The doserate varied between 0.63 – 1.43 µSv/h.
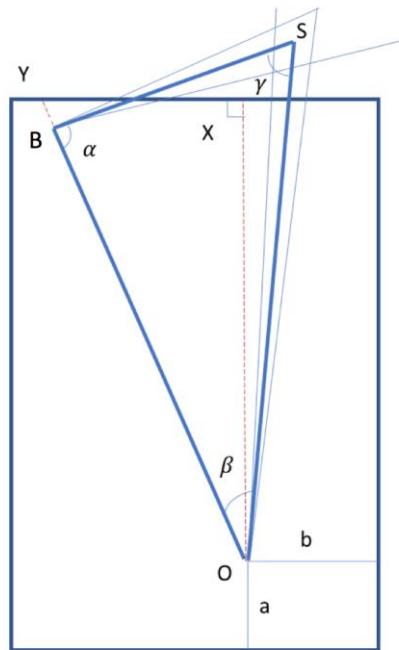

Figure 7.7. Localization of the ^{137}Cs source. RanidSOLO provided the directional angles: $\alpha = 73° \pm 2°$ and $\beta = 33° \pm 2°$. Therefore, the distances are BS = 7.5 m $\pm$ 0.6 m and OS= 13.2 m $\pm$ 0.5.

7.5 Characterisation of an unknown ^{60}Co source

Thickness of the shielding material

The results of the measurements on the unknown ^{60}Co source are given in Table 7.3.

Table 7.3. Unknown source identified as [60]Co. The measurement 102 was performed in position O whereas the measurement 103 was performed in position A (see Figure 7.5).

Meas ID	Livetime, (s)	Counts B E_B = 1173 keV	Counts A E_A = 1332 keV	Ratio of the peak areas (A/B)	Relative uncertainty of B, %	Relative uncertainty of A, %	Combined uncertainty of A/B %
102	224.9	1073.2	870.4	0.811	3.5	3.6	5.02
103	167.6	746.0	588.1	0.789	4.2	4.4	6.08

The peak area ratio (A/B) is very low (<0.9) which, according to the calibrations, means that the source is not shielded. The explanation of the low value for the ratio A/B is unknown. A good candidate, however, is the impact of the environment. The calibrations were performed at a distance of 10 m whereas the source-detector distances were much shorter in the present analysis (5.5 m and 6.2 m)

Activity estimation

The activity calculation is straightforward because the source is unshielded and the source-detector distances were measured by Environics RanidSOLO. The average activity from the two measurements is **10.6 MBq.** The two values differ from each other by 13% which is more than twice as large as predicted by the statistical uncertainty of the counts acquired. The detailed uncertainty analysis is beyond the scope of the present analysis. An educated guess is 20 - 30%.

Table 7.4. Activity analysis of the unknown ^{60}Co source. The activity was calculated from the data on the 1332 keV peak (minor interference from other peaks).

Meas ID	Source-detector distance, m	Count rate (cps) E_B = 1173 keV	Count rate (cps) E_A = 1332 keV	Activity, MBq (no shielding)
102	5.5 (OS)	4.77	3.87	9.84
103	6.2 (AS)	4.45	3.51	11.4

Comparison between nominal and measured activity

The unknown ^{60}Co source has a nominal activity of **18 MBq**. The nominal activity is not known accurately. It is fully probable that it has an uncertainty of 10 %. The information on the source or its shielding were not available for the participants at the time of the measurement and analysis.

The measured activity 10.6 MBq is 41 % smaller than the nominal value. There are two variables that have a crucial impact on the activity calculation: (1) efficiency and (2) source-detector distance. The following analysis is intended to understand the reason for the differences.

The RanidPro200 spectrometer has its own efficiency calibration which was used in the analysis. Let us compare this calibration with the measurements using a 4.95 GBq source of FOI at a distance of 10 m.

Table 7.5. Comparison of counting efficiencies at a distance of 10 m.

Energy, keV	Count rate (cps)	ε Measured at FOI	ε RadnidPro200	Difference, %
1173	567.8	1.15E-7	1.34E-7	14.2
1332	516.5	1.04E-7	1.19E-7	12.6

Table 7.5 shows that the differences in the efficiency calibration can only explain a minor fraction (1/4) of the total difference. Therefore, the error in the source-detector distance estimation is the major factor.

RanidSOLO gave fairly small uncertainties for the distance, of the order of 0.5 m (see Figure 7.5). However, the measured source-detector distances were also short, 5.5 m and 6.2 m. Therefore, in the activity estimation the 0.5 m uncertainty translates to a maximum error of 19.0%. It is likely that the error in the distance estimation is larger, of the order of 1 m. Then the calculated activity would differ from the true value by 39.7 % which is consistent with the observations.

In conclusion, the accuracy of the distance estimation plays the crucial role in the activity analysis. A 20% distance error is more than 40% error in activity estimation. Good efficiency calibration is also important.

7.6 Characterisation of an unknown ^{137}Cs source

Thickness of the shielding material

Table 7.6 shows the basic data for the step ratio analysis of the 661 keV peak of ^{137}Cs.

Table 7.6. Unknown source identified as ^{137}Cs. The measurements 104 and 105 were performed in position O and position B, respectively (see Figure 7.7).

Meas ID	Livetime (s)	Step (1/keV)	Uncertainty of step, %	Peak area	Uncertainty of peak area, %
104	163.1	41.3	13	9182	1.1
105	135.9	77.1	9.5	22099	0.7

Table 7.7. Results of the shielding analysis for the ^{137}Cs source, assuming different materials.

Shield thickness (cm) and					
attenuation factor *F(E*$_A$*)* or transmission % (in parenthesis)					
Meas ID	Source-detector distance, m	Step ratio	Pb	Fe	Concrete
104	13.2 (OS)	0.0047	2.2 (6.19)	2.5 (23.6)	9.7 (17.2)
105	7.5 (BS)	0.0032	1.3 (19.3)	1.5 (42.1)	5.7 (35.5)

Table 7.7 shows that the source is shielded but it is very difficult to say what the shielding material is. The results vary considerably at the two measurement points. There may be two reasons for this. (1) Both measurements could be correct (within statistical limits); the shielding geometry, including the material thicknesses, would then be different towards different directions. (2) The calibrations were made at a distance of 5 m and, the impact of the source-detector distance was not analysed. Therefore, we may assume that the measurement 105 is more accurate suffering less from the unknown scattering in a different measurement geometry. The best estimate for the shielding is concrete with a thickness of 5.7 cm.

Activity estimation

The results of the activity determination are given in Table 7.8. The two activity values differ from each other more than by a factor of 2. However, the measurement 105 which is nearer the calibration geometry can be considered to be more reliable. Therefore, the final result is **1.4 GBq**. Also, there is no evidence that the shield would be concrete; equally well it could have been Pb, Fe or any other material. The material uncertainties would increase the activity uncertainty estimate by a factor of 2 (see measurement 105, Table 7.7). The detailed measurement uncertainty analysis is beyond the scope of the present analysis. An educated in guess is 30-50%.

Table 7.8. Activity analysis of the unknown ^{137}Cs source, assuming a concrete shield. The analysis is based on the 661 keV peak. Measurement 105 is preferred because its source-detector distance is nearer the calibration geometry (5 m).

Meas ID	Source-detector distance (m)	Count rate (cps)	Apparent activity (GBq)	Concrete, cm	F(661)	Estimated activity, (GBq)	Accept
104	13.2 (OS)	55.8	0.528	9.7	0.172	3.07	No
105	7.5 (BS)	176.3	0.511	5.7	0.355	1.44	Yes

Comparison between nominal and measured activity

The unknown ^{137}Cs source has a nominal activity of **1.8 GBq** and is shielded with 5 cm concrete. The nominal activity is not known accurately. It is fully probable that it has an uncertainty of 10 %. The information on the source or its shielding were not available for the participants at the time of the measurement.

The measured activity 1.4 GBq is 22 % smaller than the nominal value. There are three variables that have a crucial impact on the activity calculation: (1) efficiency, (2) source-detector distance and (3) shielding. The uncertainty of the efficiency is about 10% and the shielding error is 12% (5.7 cm vs 5 cm of concrete). These two factors explain fully the difference between the measured and nominal activity. Therefore, in this case the location accuracy and precision should be fairly good (see Figure7.7)

In conclusion, the properties of an unknown source in an unknown shielding in an unknown location can be revealed. The prerequisites for success are good efficiency calibration, source localization capability and careful step ratio calibration as a function of shield thickness. The present analysis was a feasibility study. All calculations were interactive based on small MATLAB scripts. In future, the method should be made robust with more precise calibrations and furthermore, automated analysis software should be developed.

8. NaI measurements

8.1 Detection system

The measurements with NaI were performed by the Icelandic team. The detection system is called SPARCS and consists of two NaI crystals with a total volume of 4 L. The resolution at 661 keV were 7.5% and 6.8% when they were made in 2012 and 2013, respectively. At the time of the measurements the combined resolution was 56 keV at 661 kev (8.46%).

The system is made for mobile measurements and was not the best choice for the planned measurements. The resolution is much worse than for HPGe and LaBr$_3$ based system, and the volume much larger. The reason for bringing this system was twofold. The Icelandic team is also involved in NKS AUTOMORC and spectra from shielded strong sources is of interest in that project and bringing another HPGe detector would not add much to the project.

The software used is called AVID and collects spectra every second but can be summed up and exported for further analysis in other softwares.

8.2 Analysis of the ratio of the baseline step to peak area

Because of the high counting sensitivity, the SPARCS system was kept at a long distance (15-70 meters) from the sources to avoid too long dead time. Because of the altered counting geometry, it happened that people obscured the line of sight between the source and the detector. This was easily visible in the software and could be exclude in the summation spectra for each measurement. The system has an auto stabilization with a small internal source of ^{40}K. The auto stabilization had to be turned off when the ^{60}Co source was measured. These difficulties meant that the Icelandic team not successfully could do all the measurements.

The geometry of the material around the source can have a considerable effect on the spectra as is shown in Figure 5.4. This makes it very challenging to do step ratio analysis using a detector with poor resolution.

The measurements (for the ID numbers, see Appendix 1) were made 15.5 meters away from the source but the background was taken at a different location 10 meters away from the source. For the H(E,t) calculation, the counts were taken from the energy interval of 570 keV to 590 keV. That area was relative flat in the spectra used in the analysis. The step ratio was successfully measured for ^{137}Cs with steel and concrete as the shielding material. Measurement no. 8 (^{137}Cs and 4.5 cm Fe) was unusable because of interference of people being in between the detector and the source. The 662 keV peak was too weak in measurement 11. In the step analysis, measurement no. 10 is an outlier and was excluded from the least square fit. It might be due to ^{137}Cs background; the background measurement was not taken exactly at the same location as the measurement (5 meters apart, in similar surroundings).

Table 8.1. Step ratio parameters for the 662 keV peak of ^{137}Cs. Measurement @ 15.5 m, Linear function: SR = p1*x+p2. Variable *x* (thickness) in units of cm; 95% confidence interval in parenthesis.

Material	p1 (1/cm) (x 10⁻³)	p2 (x 10⁻³)
Fe	2.13 (1.39-2.88)	1.61 (0-3.83)
Concrete	0.32 (0-0.82)	2.32 (0-5.57)

9. Comparison of the results between different detectors

The step ratio for the 662 keV peak of ^{137}Cs was analysed using four different approaches: measurements with HPGe, LaBr$_3$, NaI and by simulations with Geant4. The results are shown in Table 9.1. The measurements and Geant4 simulations agree well for the slope (p1) of the response, whereas the constant (p2) parameters differ considerably. This is explained by the fact that the scattering from the environment, which was not studied in the simulations in this work, dominates the constant value whereas the slope is mainly the property of the scattering from the source shielding.

Table 9.1. Step ratio parameters for 661 keV peak of ^{137}Cs. Measurement @ 5 m, simulation in air @ 0.5 m. Linear function: SR = p1*x+p2. Variable x (thickness) in units of cm. Two germanium detectors.

Material	p1 (1/cm) (x 10^{-3})				p2 (x 10^{-3})			
Detector	HPGe	LaBr$_3$	NaI	Geant4	HPGe	LaBr$_3$	NaI	Geant4
U	-	-	-	2.5	-	-	-	0.16
Pb	-	1.65	-	1.7	-	1.0	-	0.15
Fe	1.34 1.27	1.53	2.13	1.3	2.00 1.52	0.85	1.6	0.17
Concrete	0.37 0.34	0.38	0.32	0.43	1.85 1.42	0.99	2.3	0.18
Water	-	-	-	0.20		-	-	0.18

The parameter p2 should be constant for one type of detector, simply because it is the step response at zero attenuating material between the detector and the source. Table 9.1 shows, however, considerable variability indicating that better analysis methods have to be developed. The simulation results seem to be consistent with each other, although being far away from the real measured values. Further studies are warranted to understand the impact of the environment on the response parameters.

10. Discussion

The results of the project are an important step towards improving Nordic capabilities in response to a potential radiological or nuclear security event. A new approach has been identified in order to analyze the properties of an unknown radiation shield. Two methods were identified: step ratio and peak area ratio.

The step ratio method for the shield analysis is based on scattered photons which have lost little energy and thus behave in the shield in the same way as the original photons emitted by the source. The scattered photons manifest themselves as a step near a peak, at its left side. Therefore, these photons are the markers of the shield, not the properties of the detector. The present results show that at large energies (> 600 keV), the step height (1/keV) underneath a peak is about 0.1% - 1% from total counts in the peak itself. Therefore, good tools should be available to analyse the step height correctly, and simultaneously with the peak itself. The step analysis should use counts very near the peak (10 keV). This can only be done with HPGe. The step analysis can also be performed at a larger energy interval using lower resolution detectors, such as LaBr$_3$ and NaI, but then special care must be taken to avoid interference with the peak of interest and other confounding factors, such as peaks from other nuclides or their Compton edges.

The peak ratio method is well known. However, it does not work for single line emitters, such as ^{137}Cs. Data processing is also more challenging than expected at first. Namely the narrow beam approximation is not valid for large material thicknesses, and therefore, the attenuation calculation gets more complex. Calibration measurements are necessary for different attenuating materials or a comprehensive set of Monte Carlo calculations need to be performed. The biggest challenge of the peak ratio method is the uncertainty analysis. For Co-60, better than 10% control of all uncertainties involved is required; otherwise the shield analysis gets out of hands.

The source localization capability is of utmost importance for the activity calculation. Recently a few innovative methods have emerged. The devices give the direction of the source relative to the detector. When two or more measurements are made at different locations, the source position can be determined. The method does not suffer from different attenuation to different directions. In the present study, a commercial source localizer was briefly tested; the accuracy of the system seemed to be a few degrees. Two case studies were made; the results were promising providing reliable information on source-detector distance to be used for the activity calculation of unknown sources.

Potential users of the results are the radiation protection authorities and radiation safety experts in nuclear facilities.

Appendix 1: Measurement campaign in FOI

Umeå, 9-10 Aug 2017

The measurements were performed under field conditions in a large tent, 15 x 10 m² with a concrete floor. All measurements are labelled with a running number. This primary refers explicitly to a specific measurement arrangement.

Day 1

1 Background measurement

Cs-137 measurements @ 5 m, nominal activity 1.76 GBq

2 Cs source + 0 shield	7.6 uSv/h
3 Cs + 1.85 cm Pb	1.6 uSv/h
4 Cs + <u>unknown lead shield</u>	0.16 uSv/h
5 Cs + 1 cm Fe	5.6 uSv/h (density 7.8 g/cm3)
6 Cs + 2 cm Fe	3.8 uSv/h
7 Cs + 3 cm Fe	2.7 uSv/h
8 Cs + 4.5 cm Fe	1.7 uSv/h
9 Cs + 5.5 cm Fe	1.3 uSv/h
10 Cs + 7.1 cm Fe	0.96 uSv/h
11 Cs + 8.7 cm Fe	0.80 uSv/h
12 Cs + 5 cm concrete	4.2 uSv/h, density 2.2 g/cm3
13 Cs + 10 cm concrete	2.5 uSv/h

Co-60 measurements @ 10 m, nominal activity 4.95 GBq

14 Co + 0 shield	20 uSv/h,
15 Co + 5 cm Pb	2.0 uSv/h

Day 2

Co measurements continued @ 10 m, nominal activity 4.95 GBq

21 Co + 2.5 cm Pb	6.2 uSv/h
22 Co + 10 cm Pb	0.77 uSv/h
23 Co + 1 cm Pb	14 uSv/h
24 Co +12.7 cm H2O	12.9 uSv/h
25 Co +20.3 cm H2O	8.5 uSv/h
26 Co +33.0 cm H2O	5.1 uSv/h
27 Co + DU 2.7 mm	15.9 uSv/h
28 Co + 20.3 cm H2O	9.4 uSv/h (repeated setup 25)

29 Co +12.7 H2O	12.9 uSv/h (repeated set up 24)
30 Co + 1 cm Fe	16.4 uSv/h
31 Co + 3 cm Fe	9.7 uSv/h
32 Co + 5.5 cm Fe	4.8 uSv/h
33 Co + 8.7 cm Fe	2.3 uSv/h

Eu-152 @ 5 m, nominal activity 585 MBq

34 Eu 0 cm	5.2 uSv/h
35 Eu 1.0 cm Fe	3.4 uSv/h
36 Eu 3.0 cm Fe	1.7 uSv/h
37 Eu 5.5 cm Fe	0.95 uSv/h

Two unknown sources

The participants do not know the characteristics of the sources; also their location and shielding are unknown. Two sources were placed somewhere outside the measurement tent.

101-103 source number 1

104-105 source number 2.

Appendix 2: Details of measurements with HPGe (Sweden)

(A) Step analysis with a Cs-137 source and attenuating materials (Fe, concrete) near the source. The source-detector distance was 5 m.
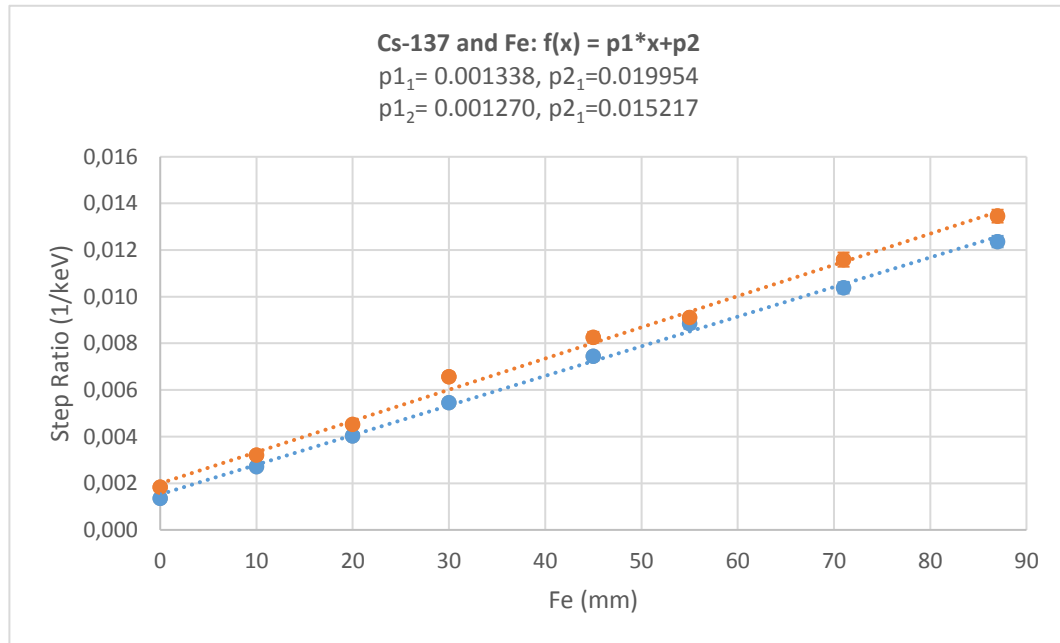
Figure 1. Step analysis with ^{137}Cs and Fe shielding. Measurement ID 2, 5-11. The two detectors are shown separately.
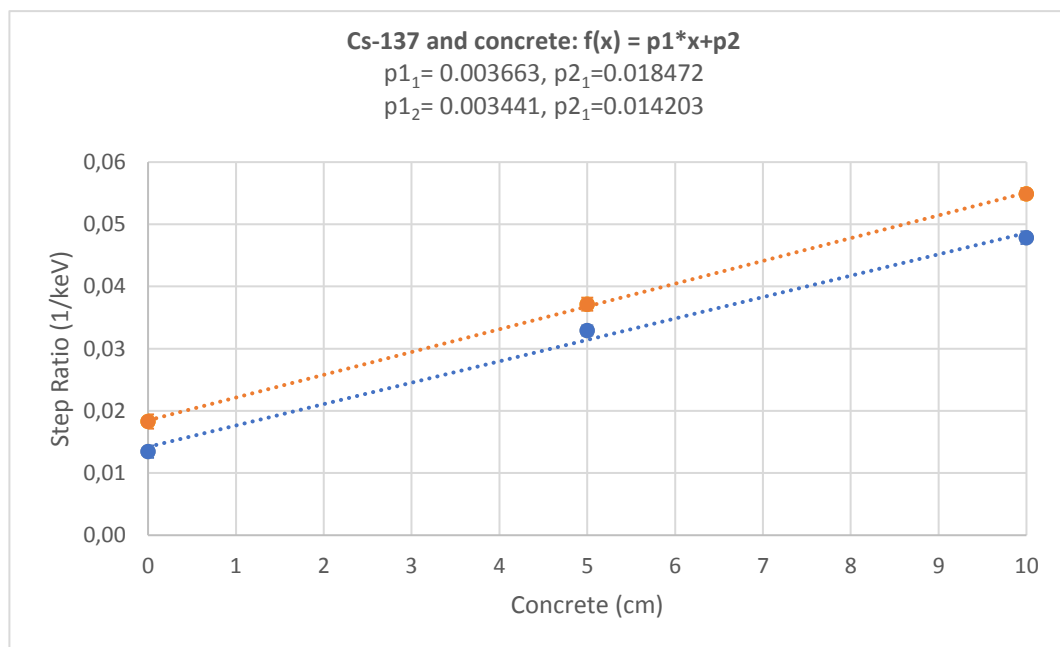
Figure 2. Step analysis with ^{137}Cs and concrete shielding. Measurement ID 2, 12, 13. The two detectors are shown separately.

(B) Step analysis with a Co-60 source and attenuating materials (Fe, water, Pb) near the source. The source-detector distance was 10 m.
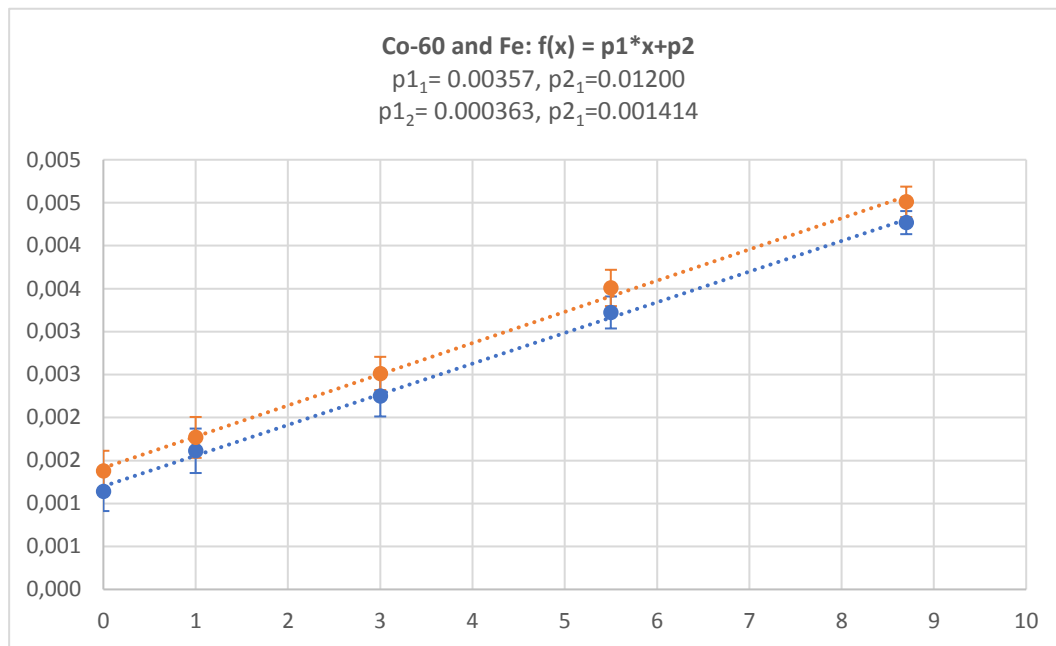
Figure 3. Step analysis with Co-60 and Fe shielding. Measurement ID 14, 30-33.

Figure 4. Step analysis with Co-60 and water shielding. Measurement ID 14, 24-25, 28

40

Co-60 and Pb: f(x) = p1*x+p2
$p1_1$= 0.000375, $p2_1$=0.001430
$p1_2$= 0.000379, $p2_2$=0.001217
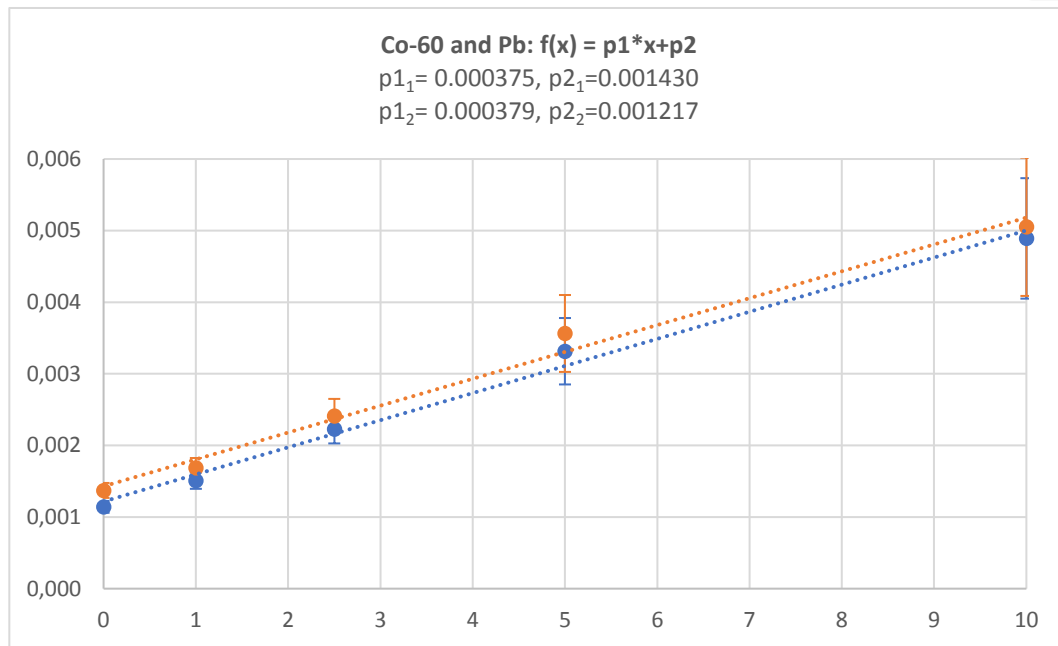
Figure 5. Step analysis with Co-60 and Pb shielding. Measurement ID 14, 15, 21-23

(C) Peak area ratio analysis with a Co-60 source and attenuating materials (Fe, water, Pb) near the source. The source-detector distance was 10 m.

Co-60 and Fe: a*exp(b*x)
a_1=0.9011, b_1=0.00270
a_2=0.9096, b_2=0.00256
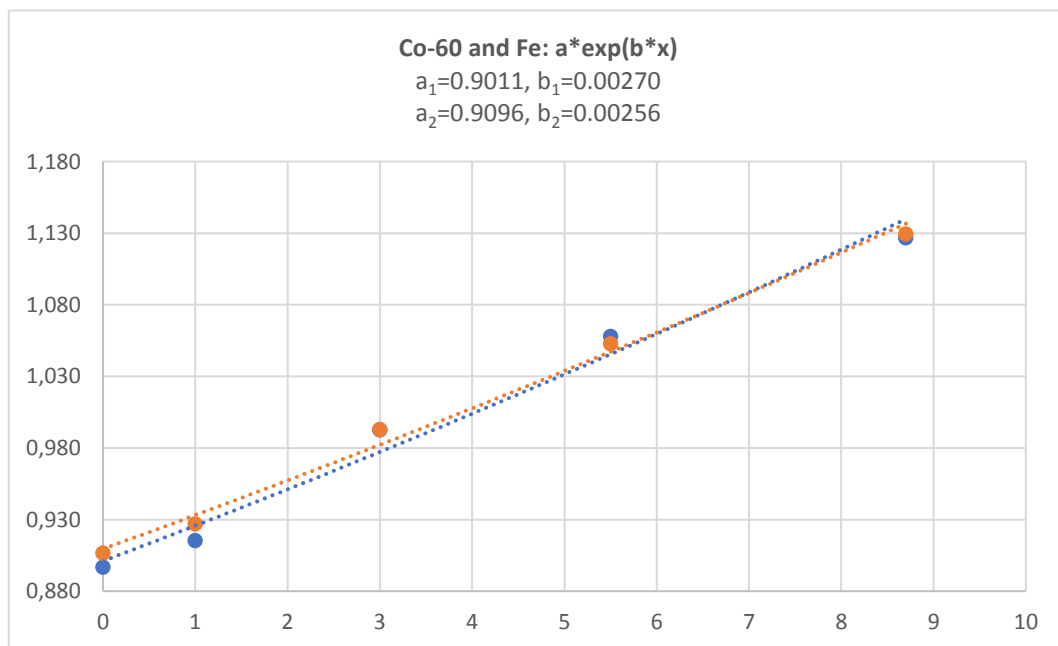
Figure 3. Peak area ratio for Co-60 and Fe shielding. Measurement ID 14, 30-33.
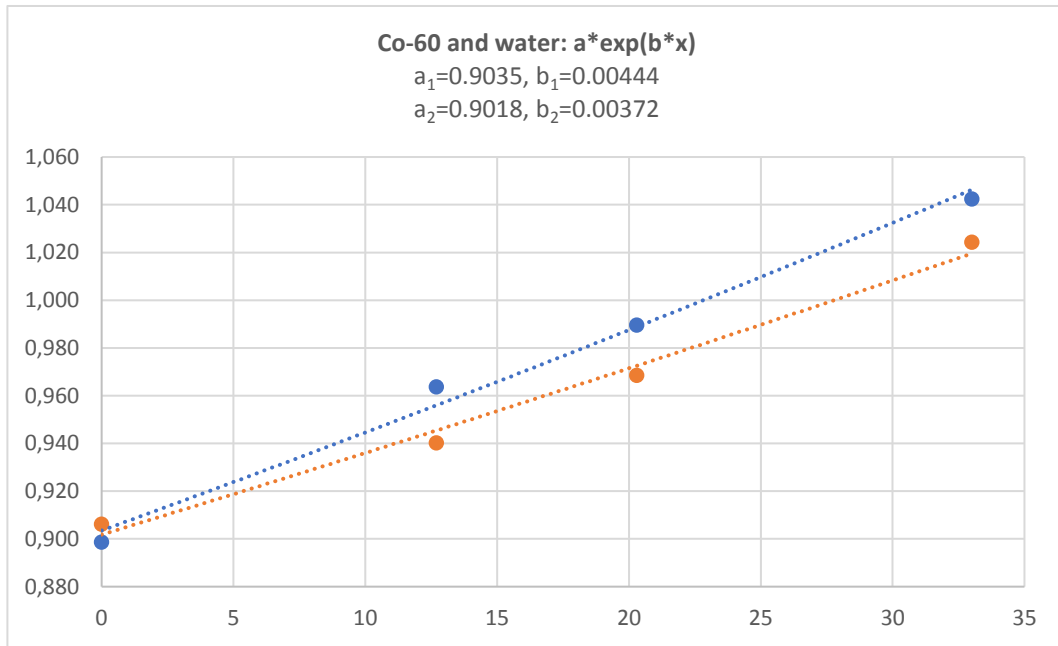
Figure 4. Peak area ratio for Co-60 and water shielding. Measurement ID 14, 24-25, 28.
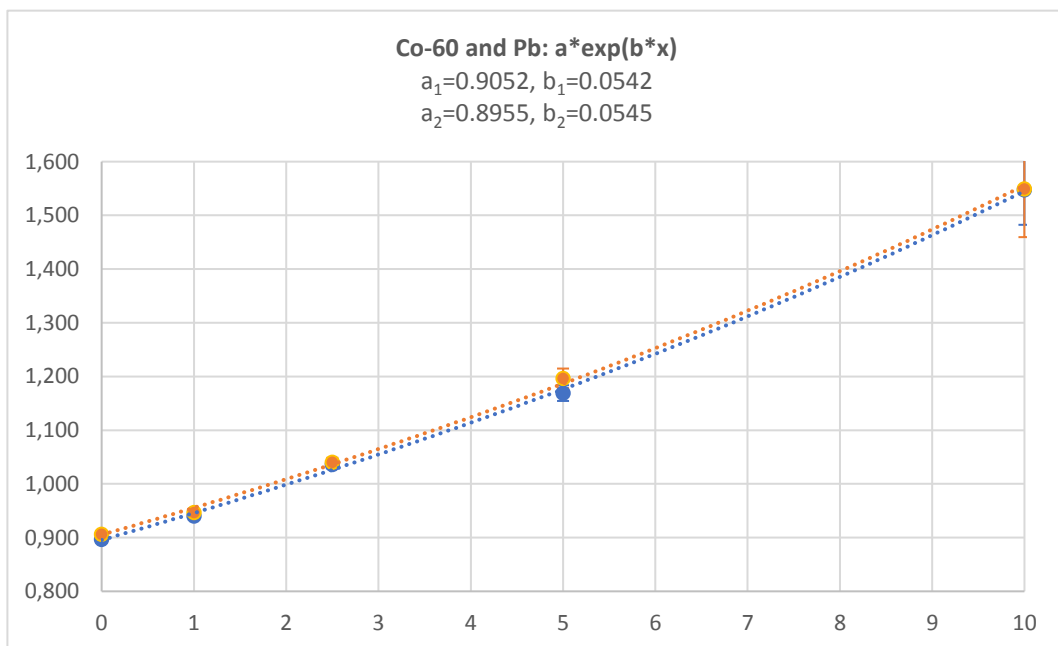
Figure 5. Peak area ratio for Co-60 and Pb shielding. Measurement ID 14, 15, 21-23

(D) Peak area ratio analysis with a Eu-152 source and attenuating material (Fe) near the source. The source-detector distance was 5 m.
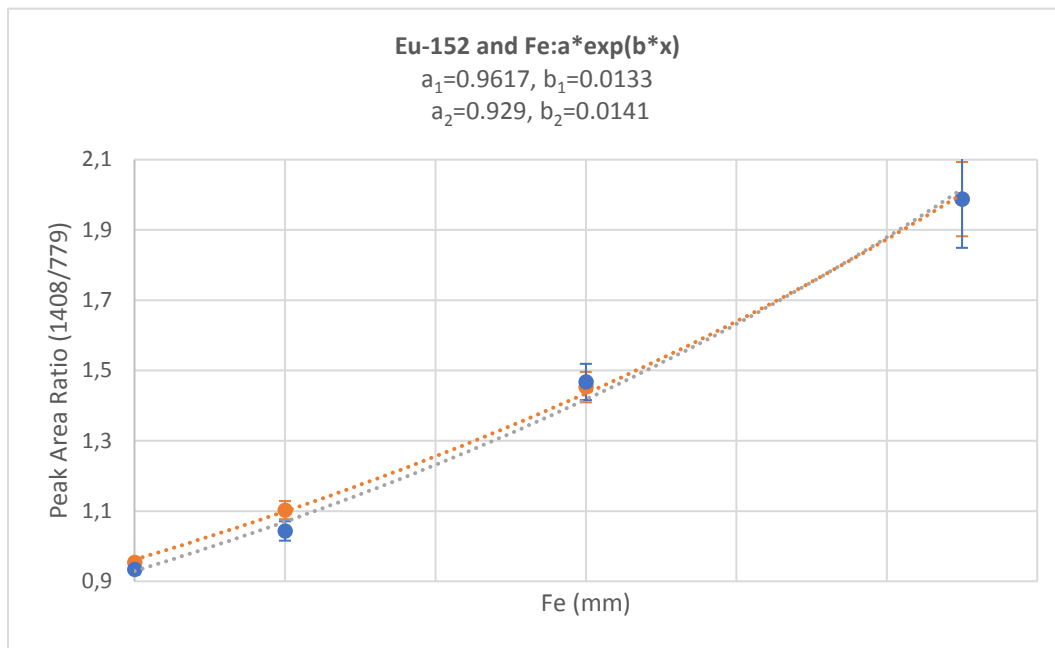
Figure 6. Peak area ratio for Eu-152 and Fe shielding. Measurement ID 34-37.

Appendix 3: Details of measurements with LaBr3 (Finland)

(A) Step analysis with a Cs-137 source and attenuating materials (Fe, Pb, concrete) near the source. The source-detector distance was 5 m.
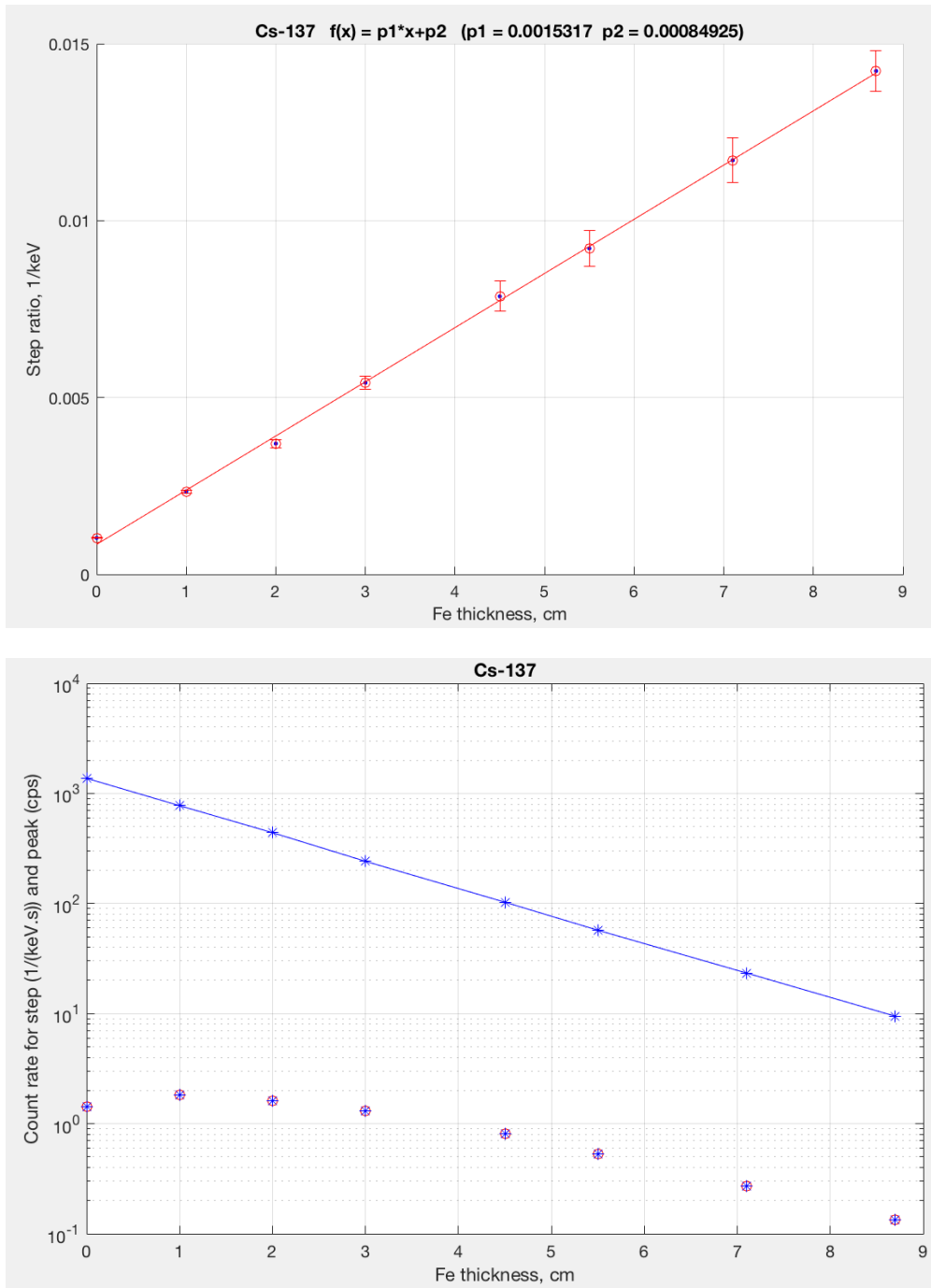
Figure 1. Step analysis with Cs-137 and Fe shielding. Measurement ID 2, 5-11. The peak count rate must be perfectly exponential as a function of shield thickness (quality assurance). Similar analysis was made for all measurements (results not included in other cases).
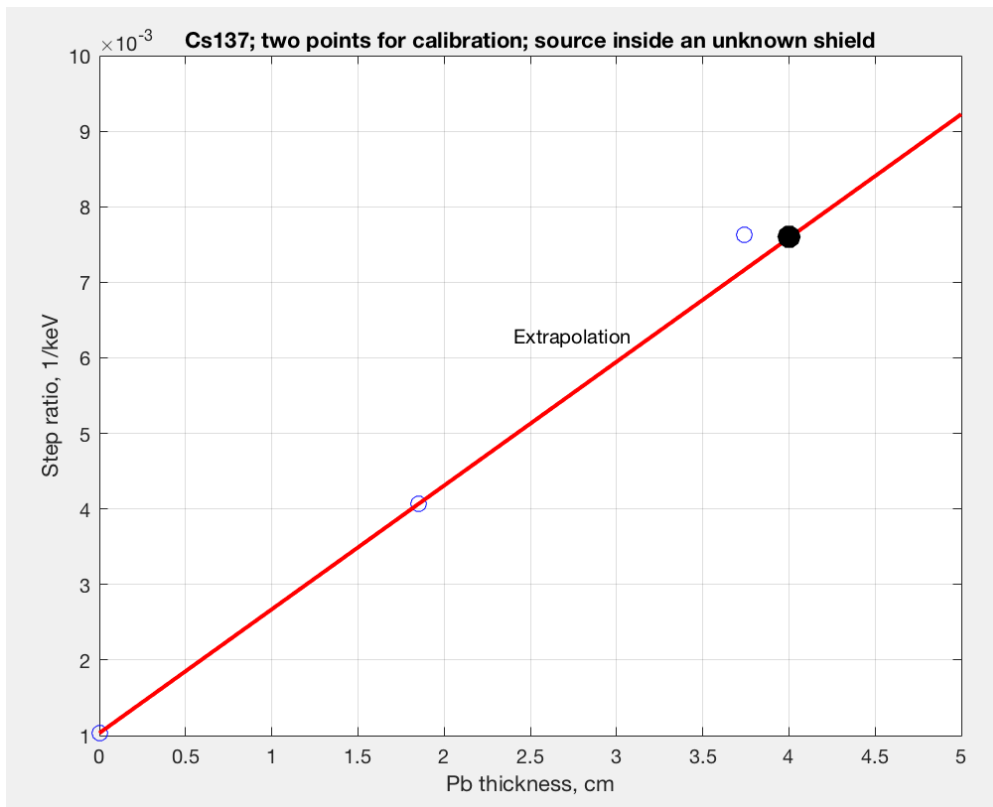
Figure 2. Step analysis with Cs-137 and Fe shielding. Measurement ID 2, 3. Only two data points are available for the calibration curve (Pb of 0 and 1.85 cm). The validity of the method was tested by analysing the thickness of an unknown cylindrical Pb shield. The step ratio was measured and then the thickness was calculated from the calibration curve. The extrapolation gives a result of 4.0 cm (black dot). The open circle refers to RaniPro 200 on-line analysis based on apparent activities which were estimated from the two calibration measurements.
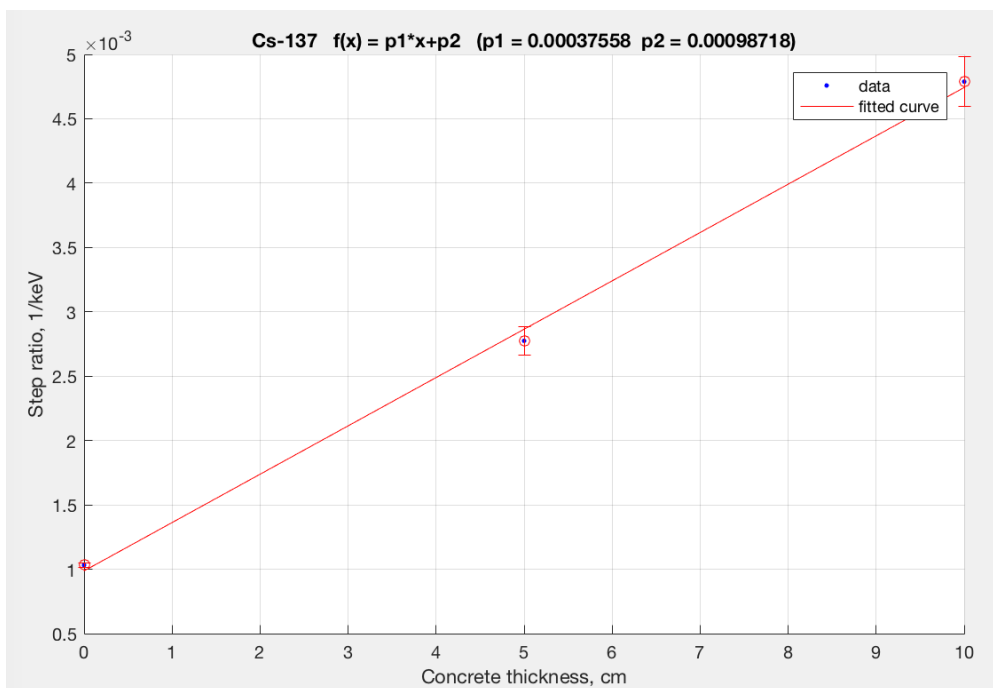
Figure 3. Step analysis with Cs-137 and concrete shielding. Measurement ID 2, 12, 13.

(E) Step analysis with a Co-60 source and attenuating materials (Fe, water, Pb) near the source. The source-detector distance was 10 m.
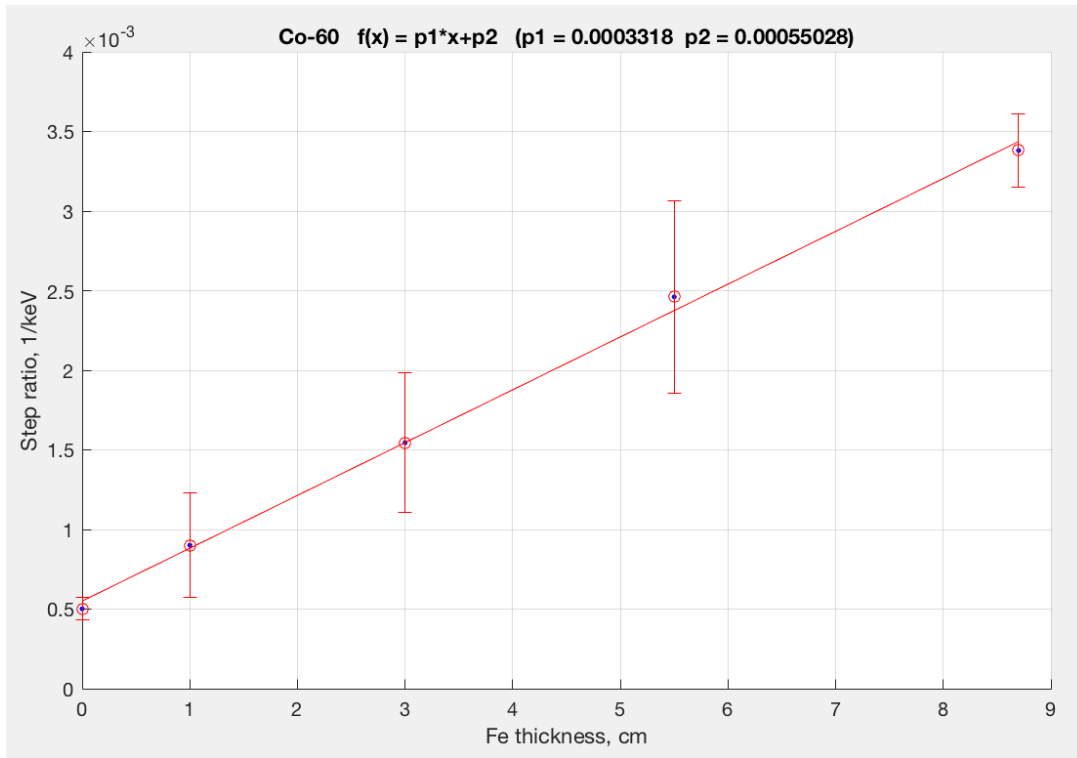

Figure 4. Step analysis with Co-60 and Fe shielding. Measurement ID 14, 30-33.
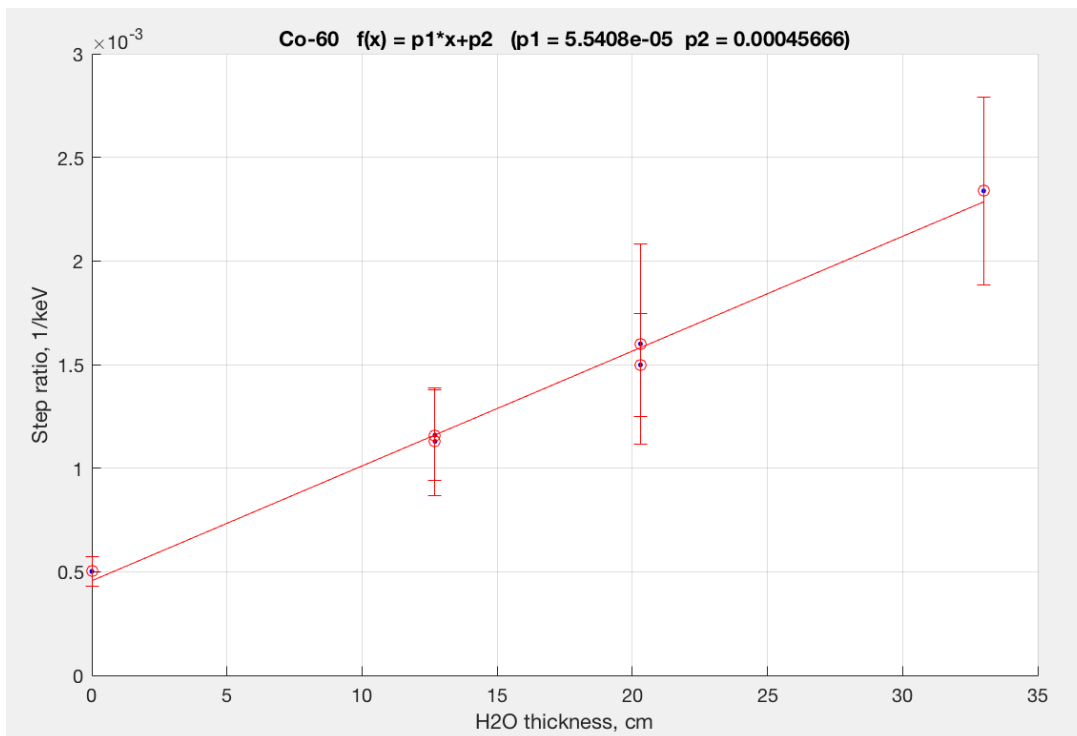

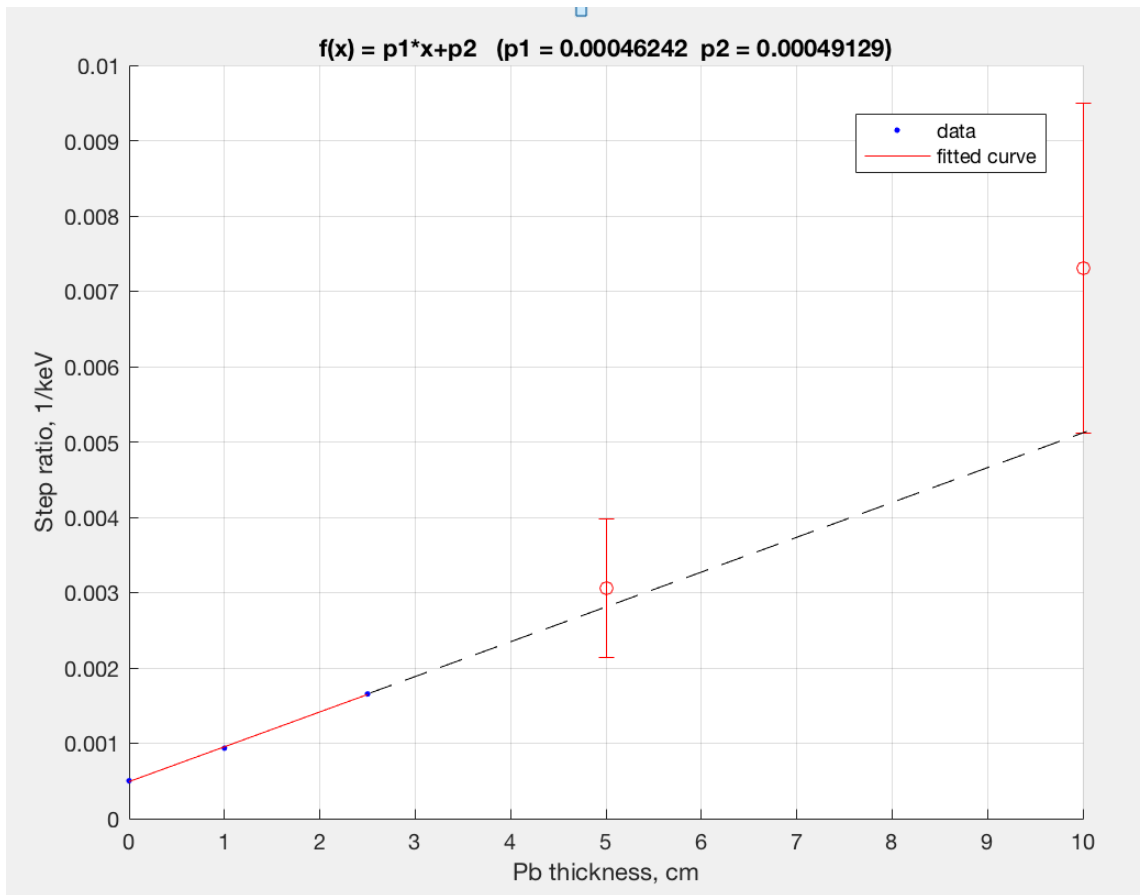Figure 5. Step analysis with Co-60 and water shielding. Measurement ID 14, 24-26, 28, 29.

Figure 6. Step analysis with Co-60 and Pb shielding. Measurement ID 14, 15, 21-23. The statistical uncertainty of the first three points is below 5% (step height 100 - 200 counts and peak area uncertainty < 0.5%). The last two points have an uncertainty of 30% (step height around 20 - 50 counts and peak area uncertainty about 2%. The fit covers only the first three points.

(F) Analysis of peak area ratio (1332/1173) with a Co-60 source and attenuating materials (Fe, water, Pb) near the source. The source-detector distance was 10 m.
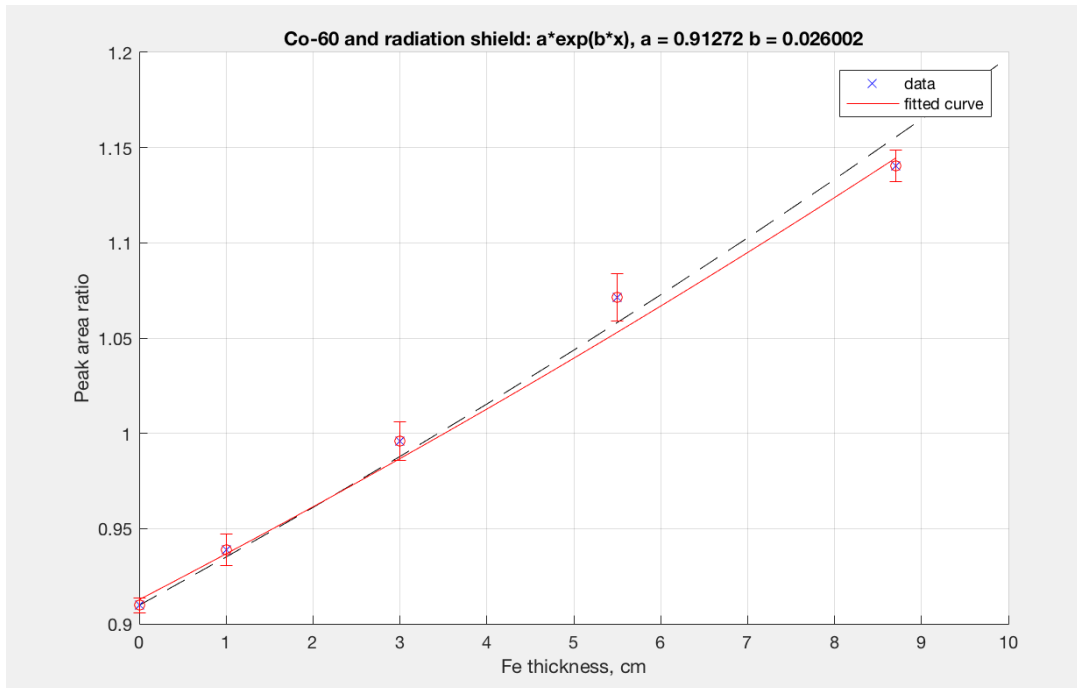

Figure 7. Peak area ratio for Co-60 and Fe shielding. Measurement ID 14, 30-33. The dashed line is the expected response function based on the NIST data.
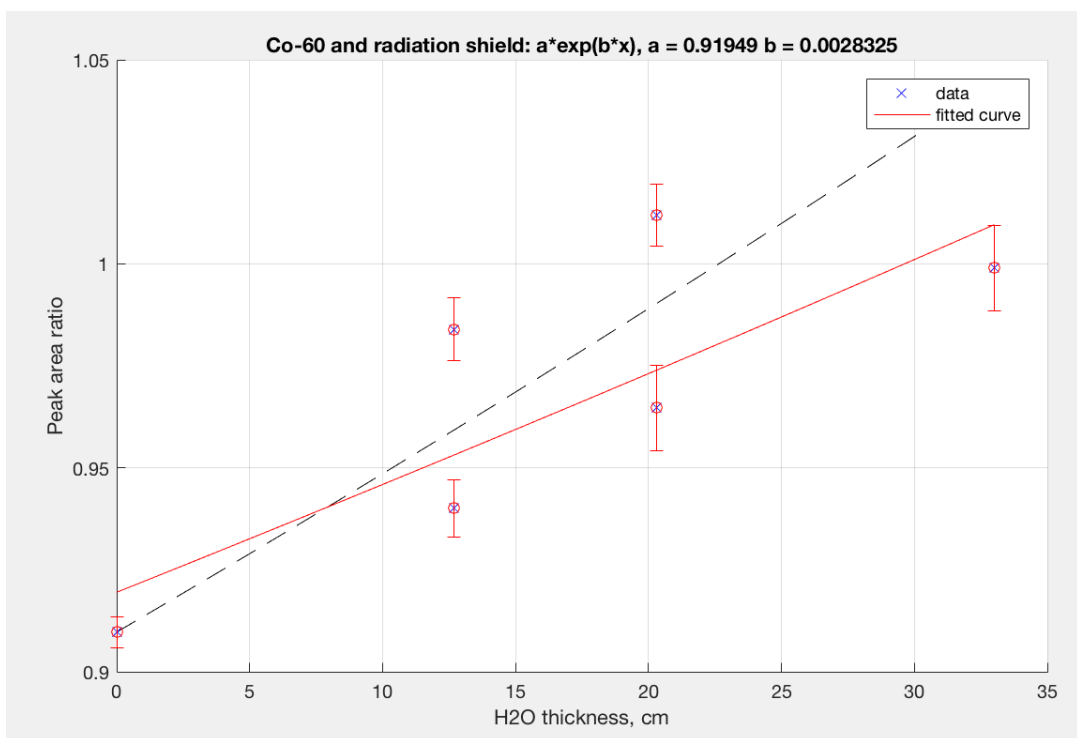

Figure 8. Peak area ratio for Co-60 and water shielding. Measurement ID 14, 24-26, 28, 29. The measurements with water thickness of 12.7 cm and 20.3 were performed twice with some configurational changes. The reason of the variability is unknown and requires further studies (the lower data set would give perfect linearity).
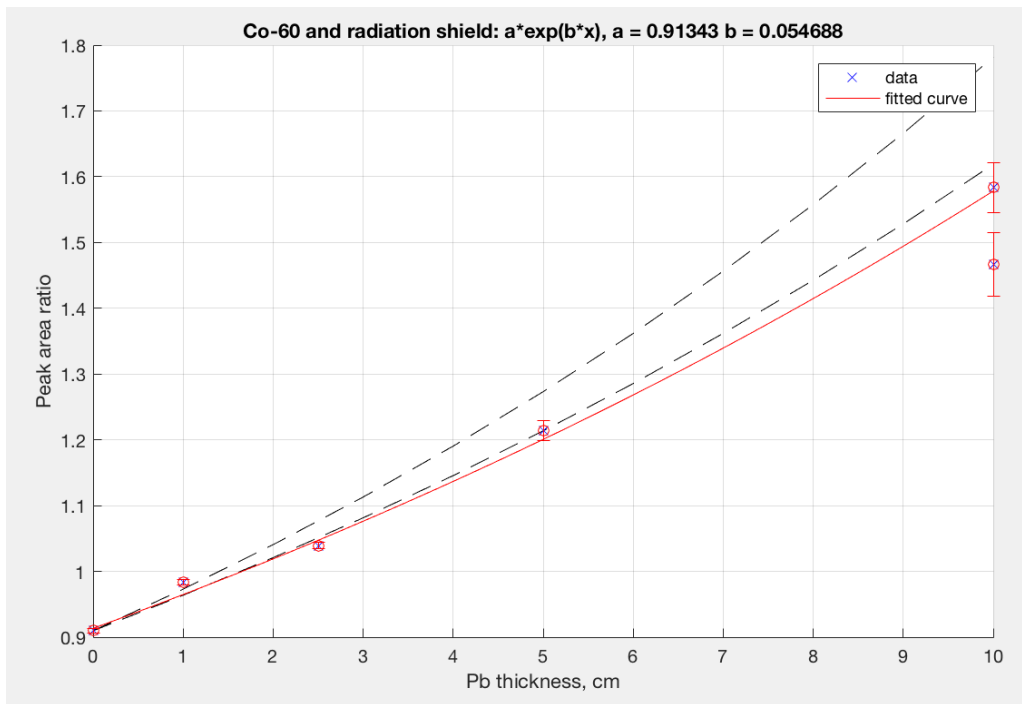
Figure 9. Peak area ratio for Co-60 and Pb shielding. Measurement ID 14, 15, 21-23. The peak areas up to the thickness of 5 cm (first four points) refer to high counting statistics (uncertainty below 1%) and therefore no background analysis was performed. However, at 10 cm of Pb the background counts due internal contamination of LaBr$_3$ detector are of the same order of magnitude as the true Co-60 counts. The lower data point at 10 cm refers to peak analysis without background subtraction, and was not included in the data fit. The upper dashed line, the expected ratio, based on total attenuation data of NIST for a narrow beam, deviates much from the measured values. However, the lower dashed curve, based on broad beam data (Rayleigh scattering excluded), is close to the measurements.

Appendix 4: Details of measurements with NaI (Iceland)

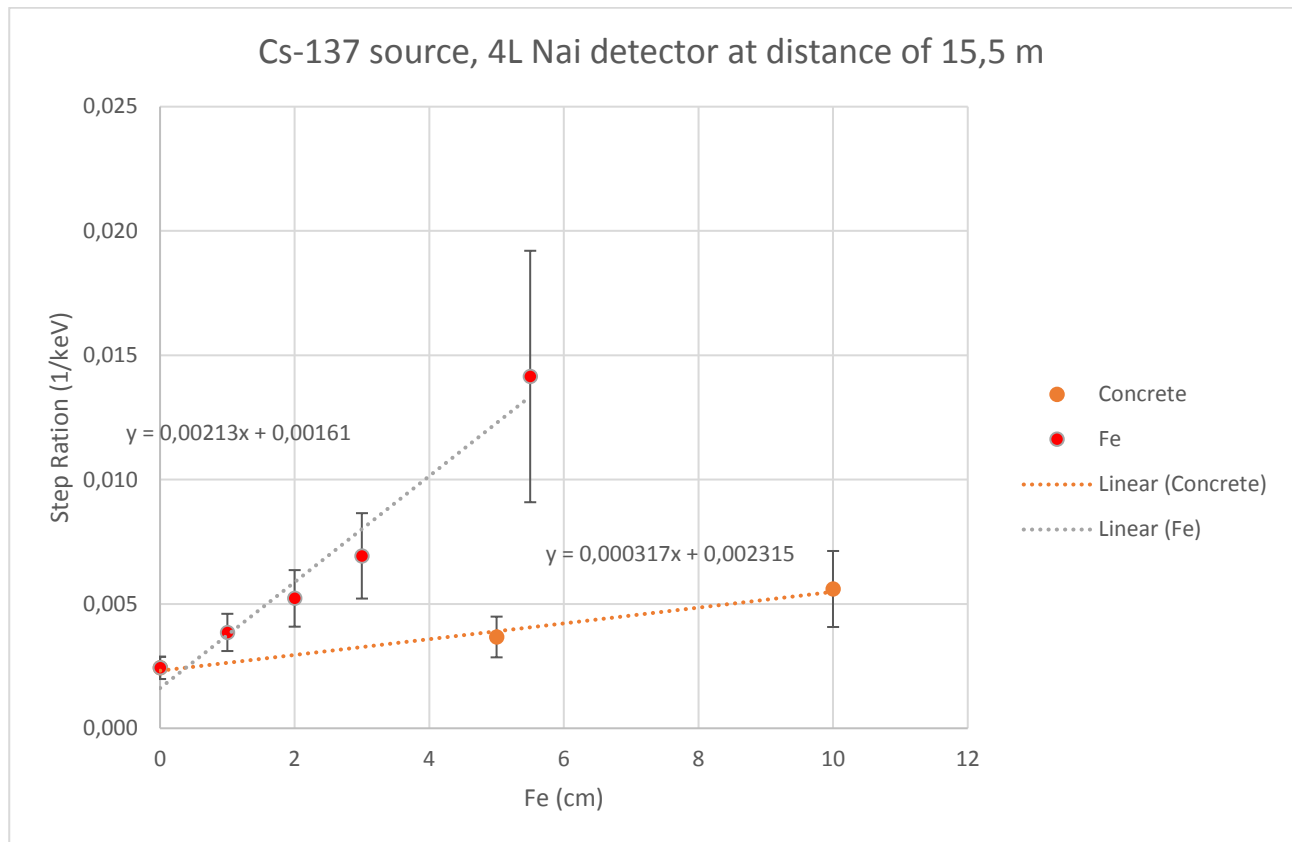**(A) Step analysis with a Cs-137 source and attenuating materials (Fe, and concrete) near the source.**

Figure 1.

Title	Activity estimation of shielded or hidden radionuclides in emergency conditions
Author(s)	[1]H. Toivonen, [2]M. Granström, [2]G. Ågren, [3]G. Jónsson, [4]B. Møller, [5]P. Roos, [2]H. Ramebäck
Affiliation(s)	[1]HT Nuclear, Finland [2]FOI, Sweden [3]IRSA, Iceland [4]NRPA, Norway [5]DTU Nutech, Denmark
ISBN	978-87-7893-487-1
Date	December 2017
Project	NKS-B / RadShield
No. of pages	50
No. of tables	16
No. of illustrations	35
No. of references	3

Abstract
max. 2000 characters

To perform a threat or risk estimation related to an unknown source, the following tasks need to be performed: detection of the source, identification of the nuclides involved, source localization and shield analysis around the source (attenuation). The present study focused on the shield analysis showing that the spectrum contains enough information to determine the attenuation of the photons in a material between the source and the detector.

The research brought together Nordic experts to use different gamma spectrometers in field conditions for improving readiness in a radiological or nuclear emergency. The field campaign was carried out in the FOI premises, Umeå, in August 2017 using HPGe, LaBr$_3$ and NaI spectrometers. For the attenuation calculation, the spectra were analysed in two ways: step analysis underneath a peak for single line emitters and peak area ratio analysis for multi-line emitters.

Careful calibrations were performed with Cs-137, Co-60 and Eu-152 sources for different attenuating materials (Pb, Fe, water and concrete) at a distance of 5 m and 10 m. Excellent data sets were generated. The results showed that in all cases the step response was linear. The peak ratio method worked well too, but the uncertainty

analysis is a challenge.

The environment, the source-detector distance in particular, seems to have an impact on the step ratio (scattering). Furthermore, the comparison of the step analysis between Cs-137 and Co-60 showed that the parameters of the model have an energy dependency. These issues require more detailed studies, simulations and experimental work, before the adaption of the method for routine field work.

The measurement campaign was a great success showing that the properties of an unknown source in an unknown location in an unknown shield can be revealed in the field conditions. The results pave the way for realistic activity calculations which are the basis of risk estimation and well-justified countermeasures in emergency conditions.